Copyright

by

Meaghan Ruth Cuddy

2018

The Thesis Committee for Meaghan Ruth Cuddy
Certifies that this is the approved version of the following Thesis:

Patterns in iscoscapes and N:P stoichioscapes of the dominant seagrasses (*Halodule wrightii* and *Thalassia testudinum*) in the western Gulf of Mexico

APPROVED BY
SUPERVISING COMMITTEE:

Kenneth H. Dunton, Supervisor

Amber K. Hardison

James W. McClelland

Patterns in iscoscapes and N:P stoichioscapes of the dominant seagrasses (*Halodule wrightii* and *Thalassia testudinum*) in the western Gulf of Mexico

by

Meaghan Ruth Cuddy

Thesis

Presented to the Faculty of the Graduate School of

The University of Texas at Austin

in Partial Fulfillment

of the Requirements

for the Degree of

Master of Science in Marine Science

The University of Texas at Austin

May 2018

Dedication

This work is dedicated to the many people on whose shoulders I have stood. To the teachers and mentors who encouraged me to pursue graduate school, my friends, my brothers, and most importantly, to my parents, Ruth and Patrick. Thank you for giving me a family filled with love and laughter, supporting me along every path I have walked, and believing in me each step of the way.

Acknowledgements

This work would not have been possible without the assistance, training, support, and patience from my many mentors, lab mates, and friends at UTMSI. Thank you to Dr. Ken Dunton, who successfully guided me through graduate school, as well as my committee members, Drs. Amber Hardison and Jim McClelland, for their valuable insights and guidance. Technical, field, statistical, and emotional support was generously provided by Dr. Ryan Hladyniuk, Patty Garlough, the UC Davis stable isotope facility, Dr. Lindsay Scheef, Frank Ernst and Stan Dignum, and the Dunton lab - Victoria Congdon, Christina Bonsell, Arley Muth, Susan Schonberg, Thomas Nguyen, and our numerous undergraduates. Additional date was provided by the Mission-Aransas NERR monitoring program, TCEQ, and Joe Meiman (NPS). Kim Jackson, thank you for teaching me to be a strong field scientist and for being our lab mom. To the MSI graduate students, thank you for being my Port A family. A special acknowledgement to the Center for Coastal Studies and Harte Research Institute at Texas A&M Corpus Christi, who gave us a home when ours was blown away (and an anti-acknowledgement to Hurricane Harvey). Thank you to Gretchen Baughman, Janis Moore, Nicole Pringle, and the students of H.G. Olsen Elementary for constantly reminding me why we do this, and that science is fun. And to my family and friends far from Texas – thank you for your unwavering love, support, and kindness throughout this journey.

Abstract

Patterns in iscoscapes and N:P stoichioscapes of the dominant seagrasses (*Halodule wrightii* and *Thalassia testudinum*) in the western Gulf of Mexico

Meaghan Ruth Cuddy, M.S. Marine Sci
The University of Texas at Austin, 2018

Supervisor: Kenneth H. Dunton

Seagrasses assimilate carbon (C), nitrogen (N), and phosphorus (P) from the water column and sediment, making their tissue nutrient content an excellent bioindicator of long-term, system-wide environmental conditions. I examined the role of seagrasses as ecological indicators of water quality and nutrient loading in three Texas estuarine systems through examination of their tissue isotopic ($\delta^{13}C$ and $\delta^{15}N$) and stoichiometric (N:P) ratios over a period of five years using maps of spatial patterns in isotopic and stoichiometric regimes ("isoscapes" and stoichioscapes"). Leaf tissue samples were collected from the dominant Texas seagrasses, *Halodule wrightii* and *Thalassia testudinum,* at 567 stations during annual sampling between 2011 and 2015. Tissues were analyzed for C, N, and P content and C and N isotopic composition. Data were used to develop interpolated maps of variations in seagrass $\delta^{13}C$ and $\delta^{15}N$ signatures and N:P

ratios in the Mission-Aransas NERR, Corpus Christi Bay, and upper and lower Laguna Madre. Regions where seagrasses had significantly enriched $\delta^{15}N$ signatures, depleted $\delta^{13}C$ signatures, or elevated N:P ratios were often associated with areas of urbanization or development. This was supported by significant relationships between $\delta^{15}N$ and $\delta^{13}C$ clusters and distance from outlets draining high population watersheds. I also documented a distinct temporal shift in $\delta^{13}C$ signatures and N:P ratios across the study areas. The change in $\delta^{13}C$ signatures was particularly notable in *H. wrightii* in 2015, when $\delta^{13}C$ signatures became more depleted and N:P ratios were elevated, following an influx of freshwater and nutrients ending a three-year drought in south Texas. The spatial and temporal variation in seagrass tissue C content reported here reflects inputs of freshwater and riverine DIC as well as changes in the benthic light environment, while the N and P dynamics reported suggest that N:P ratios and $\delta^{15}N$ signatures of seagrasses on the Texas coast are accurate bioindicators of nutrient loading in these estuaries. These metrics may thus serve as early indicators of changes in water quality.

Table of Contents

List of Tables x

List of Figures xi

Introduction 1

Methods 11

Study Site 11

Seagrass Collection 11

Tissue Analysis 13

GIS Analysis 14

Statistical Analysis 16

Results 19

Isoscapes and stoichioscape patterns in *H. wrightii* 20

Spatial Analysis – *H. wrightii* in the Mission Aransas NERR/Corpus Christi Bay (MACC) 20

Spatial Analysis – *H. wrightii* in the Upper Laguna Madre (ULM) 21

Spatial Analysis – *H. wrightii* in the Lower Laguna Madre (LLM) 23

Environmental Analysis Results – *H. wrightii* 24

Isoscape and stoichioscape patterns in *T. testudinum* 26

Spatial Analysis – *T. testudinum* in the Mission-Aransas NERR/Corpus Christi Bay (MACC) 26

Spatial Analysis – *T. testudinum* in the Lower Laguna Madre (LLM) 27

Environmental Analysis Results – *T. testudinum* 29

Discussion 30

Iscoscape and Stoichioscape Reflections of Environmental Conditions 32

Human Land Use Patterns 38

Conclusions.....43

Appendix.....65

References.....82

List of Tables

Table 1. Summary of $\delta^{15}N$, $\delta^{13}C$, and N:P ratios in MACC, ULM, and LLM *H. wrightii* blade tissue. 45

Table 2. Summary of $\delta^{15}N$, $\delta^{13}C$, and N:P ratios in MACC and LLM *T. testudinum* blade tissue. 46

Table 3. Pairwise comparison of isotopic signatures of *H. wrightii* and *T. testudinum* tissues at the same station in the same year. 46

Table 4. Repeated measures ANOVA and interregional Tukey post-hoc test results, *H. wrightii.* 47

Table 5. Results of linear regression analysis of $\delta^{13}C$, $\delta^{15}N$, and N:P ratios with relevant environmental parameters, *H. wrightii*.. 48

Table 6. Repeated measures ANOVA test results, *T. testudinum*. 49

Table 7. Results of linear regression analysis of $\delta^{13}C$, $\delta^{15}N$, and N:P ratios with relevant environmental parameters, *T. testudinum*. 50

Table 8. Cluster analysis results, *H. wrightii.* 65

Table 9. Tukey post-hoc pairwise interannual comparisons for $\delta^{13}C$, $\delta^{15}N$, and N:P ratios, *H. wrightii*.. 68

Table 10. Cluster analysis results, *T. testudinum*.. 72

Table 11. Tukey post-hoc pairwise interannual comparisons for $\delta^{13}C$, $\delta^{15}N$, and N:P ratios, *T. testudinum*.. 74

List of Figures

Figure 1. Tier 2 sampling stations, Mission-Aransas estuary and Corpus Christi Bay (MACC), Upper Laguna Made (ULM), and Lower Laguna Madre (LLM). 51

Figure 2. Mean *H. wrightii* and *T. testudinum* (a, d) $\delta^{13}C$ signatures, (b, e) $\delta^{15}N$ signatures, and (c, f) N:P ratios tissues in MACC, ULM and LLM, 2011-2015.....52

Figure 3. Isoscapes and stoichioscapes of *H. wrightii* in the MACC, 2011-2015. Top: $\delta^{13}C$ signatures. Middle: $\delta^{15}N$ signatures. Bottom: N:P ratios.....53

Figure 4. Isoscapes and stoichioscapes of *H. wrightii* in the ULM, 2011-2015. Top: $\delta^{13}C$ signatures. Middle: $\delta^{15}N$ signatures. Bottom: N:P ratios.....55

Figure 5. Isoscapes and stoichioscapes of *H. wrightii* in the LLM, 2011-2015. Top: $\delta^{13}C$ signatures. Middle: $\delta^{15}N$ signatures. Bottom: N:P ratios.....56

Figure 6. Pooled salinity readings collected during regular environmental monitoring vs. pooled *H. wrightii* $\delta^{13}C$ signatures. 57

Figure. 7. Pooled water column N concentrations (DIN SMWP data in the MACC), TN TCEQ/NPS data in the ULM and LLM) vs. pooled *H. wrightii* N:P ratios and $\delta^{15}N$ relationship with N:P ratios 58

Figure 8. Isoscapes and stoichioscapes of *T. testudinum* in the MACC, 2011-2015. Top: $\delta^{13}C$ signatures. Middle: $\delta^{15}N$ signatures. Bottom: N:P ratios. 59

Figure 9. Isoscapes and stoichioscapes of *T. testudinum* in the LLM, 2011-2015. Top: $\delta^{13}C$ signatures. Middle: $\delta^{15}N$ signatures. Bottom: N:P ratios.....61

Figure 10. Pooled salinity readings collected during regular environmental monitoring 6-8 weeks prior to plant tissue collection vs. pooled *T. testudinum* $\delta^{13}C$ signatures. 62

Figure 11. Pooled water column N concentrations (DIN SMWP data in the MACC, TN TCEQ data in the LLM) vs. pooled *T. testudinum* N:P ratios and and $\delta^{15}N$ relationship with N:P ratios 63

Figure 12. Land use across the lower/middle Texas coast with HUC-10 USGS watershed boundaries. Stars denote significant areas of enriched $\delta^{15}N$, depleted $\delta^{13}C$, and elevated N:P ratios. Regressions depict the significant linear relationships between distance from major outlets 64

Figure 13. C:N biplot, *H. wrightii* and *T. testudinum* in all regions 77

Figure 14. Environmental data collected during Tier-2 sampling vs. *H. wrightii* $\delta^{13}C$ signatures: MACC, ULM, and LLM, 2011-2015. 78

Figure 15. Pooled chlorophyll-*a* concentrations measured during regular environmental monitoring 6-8 weeks prior to plant tissue collection vs. pooled *H. wrightii* $\delta^{13}C$ signatures.....79

Figure 16. Environmental data collected during Tier-2 sampling vs. *T. testudinum* $\delta^{13}C$ signatures: MACC and LLM, 2011-2015.....80

Figure 17. Pooled chlorophyll-*a* concentrations measured during regular environmental monitoring 6-8 weeks prior to plant tissue collection vs. pooled *T. testudinum* $\delta^{13}C$ signatures at stations within 10 km (MACC) or 5 km (ULM/LLM), in (a) MACC and (b) LLM from 2011-2015.....81

Introduction

Mixed-species seagrass beds are the dominant benthic vegetative community on the south Texas coast, covering approximately 87,000 hectares of the benthos (Dunton et al. 2011). Seagrass beds provide a number of key ecological functions; they serve as habitat and shelter for benthic organisms and juvenile fish (Duarte 2002; Beck et al. 2001), function as key carbon sequestering systems (Kennedy et al. 2010; McLeod et al. 2011; Fourqurean et al. 2012), and alter water flow (Fonesca et al. 1982; Ackerman and Okubo 1993; Peterson et al. 2004; Ondiviela et al. 2014) to stabilize sediments (Gacia and Duarte 2001).

Seagrasses are also frequently used as an ecological bioindicator, signaling changes in environmental conditions (Orth et al. 2006; Montefalcone 2009). Bioindicator species are sensitive to processes that result in changes to the larger community and thus are representative of the condition of the ecosystem (Markert et al. 2003; Parmar et al. 2016). Along with responding to changes in light, temperature, and salinity, seagrasses take up carbon (C), nitrogen (N), and phosphorus (P) from both the water column and sediment porewater for use in physiological processes, and assimilate these source materials into their own tissues over time (Duarte 1990; Lee and Dunton 1999; Touchette and Burkholder 2000). This integrated signature can be tracked through plant tissues via isotopic signatures and elemental C:N:P ratios, serving as a general signal of C, N, and P sources and cycling throughout the system (Yamamuro et al. 2003; Lee et al. 2004). This process makes seagrasses a useful proxy for developing a long-term, synoptic

understanding of system-wide C, N, and P availability and inputs (Fourqurean et al. 1997). Studies in numerous regions have indicated that marine macrophyte isotopic and stoichiometric signatures can be integrated over spatial and temporal scales ("isoscapes" and "stoichioscapes") to provide an overview of C and nutrient regimes of the local system (Bowen 2010). For instance, seagrass isoscapes and stoichioscapes developed for the Bermuda platform identified regions of P-limitation and provided evidence of unique N cycling that results in highly depleted DIN pools within the system (Fourqurean et al. 2015).

Tools such as isoscapes and stoichioscapes are especially useful in systems where it is challenging to define the nutrient regime, such as Texas bays and lagoons. The majority of nutrient inputs to the Texas coast occur during sporadic flood events, when rivers deliver large loads of nutrients and organic material to the bays and lagoons (Onuf 2007; Reyna et al. 2017). Due to the erratic and unpredictable nature of these events, it can be difficult to typify standard nutrient conditions. Large, storm-driven fluxes of nutrients and C are inherently ephemeral, fueling temporary bursts of productivity and resulting in a large degree of variation in the ambient nutrient concentrations measured in the water column throughout the year (Hudak and Banks 2006; Mooney and McClelland 2012). Seagrass isotopic and stoichiometric signatures, integrated over time, can provide key information about the long-term bioavailable C and N pools and reflect variations in C and N supply and cycling (Hemminga and Mateo 1996; Lepoint et al. 2004). Further, studies of seagrass tissue isotopic signatures and stoichiometry have found that variations

in isotopic and stoichiometric trends over time and space are indicative of changes in water quality or environmental condition (Anderson and Fourqurean 2003; Papadimitriou et al. 2005).

The stable isotopic signatures of C ($\delta^{13}C$) and N ($\delta^{15}N$) are common isotopic tracers in aquatic systems (Fry 2006). C and N isotopic species are acquired, assimilated into tissue, and used in physiological processes at different rates due to kinetic isotope effects, and therefore can be used to define how the available C and N pools are being utilized by seagrasses (Fry 2006).

In systems where nutrient sources are well defined, spatial variations in isotopic values can reflect how plants' N needs are met (Fry 2006). $\delta^{15}N$ signatures of plant leaf tissues often reflect the known $\delta^{15}N$ signatures of N inputs, including dissolved inorganic N (DIN) derived from specific sources (Lepoint et al. 2004; Xue et al. 2009). Enriched $\delta^{15}N$ signatures have been associated with areas exposed to anthropogenic nutrient pollution such as N-enriched human sewage effluent (McClelland et al. 1997; Yamamuro et al. 2003; Costanzo at al. 2001). Fourqurean et al. (2015) used seagrass $\delta^{15}N$ isoscapes to demonstrate the presence and processing of sewage-influenced groundwater entering the Bermuda Platform, reflected in a localized N-15 enrichment at nearshore sites and a rapid depletion in $\delta^{15}N$ with distance. Similarly, plants utilizing upwelled nitrate tend to have enriched $\delta^{15}N$ signatures, while plants exhibit depleted $\delta^{15}N$ signatures as they become reliant on recycled N available via microbial processes like N-fixation (Fourqurean et al. 1997; Carriquiry et al. 2016).

$\delta^{13}C$ signatures can similarly be used to understand the DIC pool. $\delta^{13}C$ tissue signatures in estuarine plants reflect, among other things, the dissolved inorganic C (DIC) pool (Hemminga and Mateo 1996). This pool is the sum of atmospheric CO_2 exchange, carbonate equilibrium chemistry, terrestrial inputs, and biological processes. Generally, riverine sources of C are more depleted with respect to C-13 (approximately -10 ‰), which reflects contributions from carbonate and limestone weathering, terrestrial organic matter oxidation, and exchanges with atmospheric and soil CO_2. Marine sources are more C-13 enriched (approximately 0-2 ‰) due to the influence of atmospheric CO_2 exchange and calcium carbonate dissolution in the marine environment (Fry 2002; Kaldy et al. 2005; Planavsky et al. 2011; Ceburnis et al. 2016). Previous work has indicated that in estuarine systems, $\delta^{13}C$ signatures are positively correlated with salinity, reflecting a decline in the relative contribution of riverine DIC to the DIC pool with increasing distance from freshwater sources (Fry 2002; Bishop et al. 2017). Similarly, $\delta^{13}C$ signatures of *Thalassia testudinum*, a common seagrass in the Gulf of Mexico, have been shown to also reflect isotopic values of various C sources entering the DIC pool through decomposition of proximate organic matter sources; seagrasses growing near mangrove stands, for example, are more depleted in $\delta^{13}C$ than those far from mangroves, indicating the contribution of terrestrial plant-derived C to the DIC pool (Lin et al. 1991).

N isoscape and stoichioscape studies have frequently been employed to clarify nitrogen cycling and use by plants. High rates of N-fixation, for instance, leave behind a relatively $\delta^{15}N$-depleted DIN pool, while denitrification results in a relatively $\delta^{15}N$-

enriched DIN pool (Fourqurean et al. 1997; Mahaffey et al. 2003; Unkovich 2013). Seagrass tissue $\delta^{15}N$ signatures have been shown to reflect spatial shifts in the estuarine DIN pool that are the result of variations in N cycling, with plant isotopic signatures mirroring shifts across systems from a DIN pool predominantly comprised of oceanic nitrate to the domination of processes such as N-fixation and ammonification as oceanic DIN becomes less available (Carriquiry et al. 2016).

$\delta^{13}C$ signatures of seagrasses have also been used extensively to define C processing within plants as well as the environmental conditions impacting the C uptake and use. Photoassimilatory discrimination of C isotope species during photosynthesis results in discrimination against isotopically heavier C-13, as the lighter isotope can be more rapidly taken up and utilized. However, under high light conditions, increased photosynthetic rates result in a reduction of this discriminatory uptake (Cooper and DeNiro 1989; Lepoint et al. 2003). Therefore, seagrass $\delta^{13}C$ signatures become more enriched with higher benthic light availability to reflect increasing uptake of the isotopically heavier C species, as higher irradiance leads to a reduction in fractionation of DIC during photosynthesis, though this trend can vary amongst species (Campbell and Fourqurean 2009; Fourqurean et al. 2015). A survey of *T. testudinum* in the Bahamas and Florida Keys found that C isotope signatures varied spatially with depth; $\delta^{13}C$ signatures decreased with depth as light attenuated through the water column. $\delta^{13}C$ signatures can also differ regionally due to the length of time during which photosynthetic activity was light-saturated, further indicating the that $\delta^{13}C$ signatures

reflect differences in light conditions across both spatial and temporal scales (Hu et al. 2012; McPherson et al. 2015).

Like isotopic signatures, seagrass elemental tissue content and the stoichiometric relationships between C, N, and P reflect conditions of the plants' environment. Seagrass C:N:P ratios, standardly defined as 550:30:1 (Atkinson and Smith 1984) can provide key information about nutrient availability within a system. Agreement with or deviation from this standard nutrient ratio reflects localized N or P-limitation (Burkholder et al. 2013; Fourqurean et al. 2015). Seagrass tissue N content has been shown to be indicative of the nutrient conditions in the location where the plant is growing (Lee et al. 2004). Stoichioscapes can visually represent if a system is N- or P-limited, with conditions of general N-limitation occurring when seagrass N:P ratios are below 30 and general P-limitation at ratios greater than 30 (Fourqurean et al. 2015). In California and Florida, seagrass N:P ratios reflect both seasonal and geographic changes in nutrient availability, with tissue nutrient content varying in response to spatial shifts from nearshore nutrient replete conditions to offshore N-limitation. N:P stoichioscapes also reflect temporal shifts in the composition of N and P pools related to seasonal upwelling and storm events (Fourqurean et al. 1997; Ferdie and Fourqurean 2004). This signal has important implications for detecting conditions of eutrophication as well as understanding how eutrophication will impact the seagrass community as a whole.

Along with spatial analyses that can identify key areas of C and N inputs and localized regions of isotopic depletion or enrichment, isoscapes and stoichioscapes vary

within a region from year to year. Distinct temporal changes in isoscapes and stoichioscapes can reflect important environmental events that induce temporary changes in the system, such the impact of flood events on salinity, light attenuation, and nutrient delivery, or to track changes in the ecosystem over time as human land uses change and urban, suburban, or agricultural development progresses (Sanstchi et al. 2007; Hu et al. 2012; McPherson et al. 2015). In a two year study, $\delta^{13}C$ and $\delta^{15}N$ signatures in seagrasses were shown to vary over time, with isotopic values correlated with temporal changes in primary production and the composition of the local N and C pools (Fourqurean et al. 1997).

The use of stable isotope signatures to define ecological conditions, however, is complex due to the large number of possible factors influencing the signature of a particular tissue sample. Organism isotopic signatures reflect not only a competing pool of sources (Parnell et al. 2010), but also microbial transformations (such as N-fixation, nitrification, denitrification, and ammonification) happening within the C and N pools in the environment before uptake (Tieszen 1991; Robinson 2001; Denk et al. 2017; Nikolenko et al. 2018). Adding another layer of complexity is the role of fractionation effects during metabolic processes like photosynthesis and respiration, resulting in changes to tissue isotopic signatures. (Dawson et al. 2002). Generally, as organisms acquire nutrients, elemental species that are isotopically lighter are assimilated more quickly and are more reactive, while isotopically heavier species are incorporated more slowly (Peterson and Fry 1987; Handley and Raven 1992; Fry 2006). When using

organismal isotopic and stoichiometric signatures to understand ecological conditions, it is vital to consider these many competing factors and processes that play a role in the signature of any given tissue sample.

Here, I present $\delta^{13}C$, $\delta^{15}N$, and N:P data for the dominant seagrass species, *Halodule wrightii* and *Thalassia testudinum*, in three Texas coastal bay regions over a five year period (2011-2015). I used GIS software to interpolate isoscape and stoichioscape maps to illustrate C, N and P dynamics in seagrass communities in the Mission Aransas National Estuarine Research Reserve and Corpus Christi Bay, Upper Laguna Madre, and Lower Laguna Madre. This project sought to define general trends in $\delta^{13}C$, $\delta^{15}N$, and N:P regimes along the south Texas coast and identify localized areas of depletion or enrichment in seagrass tissue $\delta^{15}N$ and $\delta^{13}C$ signatures as well as areas of abnormally high or low N:P ratios. I also sought to identify interannual variations in these dynamics that may be attributable to notable events, such as storms or floods. I used water quality data to establish relationships between seagrass isotopic signatures, stoichiometric ratios, and changes in environmental conditions induced by natural events and anthropogenic pressure. I used the USGS national land cover database (https://www.mrlc.gov/) to determine the relationship between human land use patterns and trends in isotopic and stoichiometric variations over time and space.

Based on previous studies of seagrass isotopic and stoichiometric patterns, I developed the following hypotheses:

- **Seagrass $\delta^{15}N$ and $\delta^{13}C$ signatures will spatially vary relative to human land use and both natural and anthropogenic nutrient source inputs.** It was expected that $\delta^{15}N$ signatures would be generally enriched in nearshore areas and localized enrichment would be detected in seagrasses growing at sites closely associated with human development. This trend has been seen consistently in seagrass isoscapes in other systems, indicating the nearshore influence of anthropogenic N sources. Generally, tissue $\delta^{15}N$ signatures deplete as distance from shore increases, shifting to reflect natural N cycling by the biological community of the system. It was expected that C isotope values will reflect changes in light regimes, with $\delta^{13}C$ signatures increasing in areas of higher light availability and becoming more depleted in seagrasses growing in areas of localized turbidity. It was also expected that seagrass $\delta^{13}C$ signatures would reflect distance from freshwater outlet, due to the distinct $\delta^{13}C$ signatures of riverine versus marine DIC pools.
- **N:P ratios would reflect the standard ratio for seagrasses and benthic macrophytes of approximately 30:1, with deviations possibly indicating localized nutrient limitation**. Historically the Laguna Madre and Texas coastal bays are nutrient replete systems. However, localized nutrient limitation has been observed sporadically in the region. It was anticipated that the stoichioscapes produced using seagrass N:P ratios would be able to define these areas of localized nutrient limitation.

- **Seagrass $\delta^{15}N$ and $\delta^{13}C$ signatures would temporally vary in response to events that resulted in temporary environmental perturbations.** Notable events, such as floods, deliver large ephemeral nutrient loads to the coast while at the same time altering environmental parameters like salinity. Therefore, it was expected that isoscape and stoichioscape maps would vary over time in a way that reflect these temporary shifts in water quality or nutrient pools.

This project incorporates seagrass $\delta^{15}N$, $\delta^{13}C$, and N:P signatures as an additional metric for elucidating variation in C, N, and P supply and use in coastal bay systems as well as understanding the relationships between plant tissue elemental content, water quality, and environmental conditions. Using the coastal bays and lagoons of south Texas as an example region, it highlights the important supplemental role isoscape and stoichioscapes can play in understanding the complex factors that influence C and N regimes in nearshore marine systems.

Methods

STUDY SITE

This study covers approximately 235,000 acres of benthos in the bays and lagoons along the Texas coast. Urban and suburban development in this region has increased in recent years, leading to changes in nutrient inputs into the system, particularly in regards to N and P. Five seagrass species are found along the Texas coast in both monospecific and mixed beds: *H. wrightii*, *T. testudinum*, *Ruppia maritima*, *Halophila englemanii*, and *Syringodium filiforme*. *H. wrightii* and *T. testudinum* are by far the dominant species, representing over 50% of total seagrass area. Nearly 80% of the current seagrass cover along the Texas coast is found in the Laguna Madre alone, making it a region of high ecological, economic, and recreational value. (TPWD 1999).

SEAGRASS COLLECTION

Seagrass tissue samples were collected annually between 2011and 2015 through the Texas Seagrass Monitoring program (www.texasseagrass.org). This multi-tiered monitoring approach is designed to capture short-term changes as well as long-term trends in the health of Texas seagrass beds. Tissue sample collection takes place during Tier-2 surveys, following a rapid assessment field methodology developed by Dunton et al. (2011) for 567 seagrass stations representing 94% of Texas seagrasses (Fig. 1). Sampling station locations are based on the vegetation maps produced by the 2004/2007 NOAA Benthic Habitat Assessment project and were established in 2010. A hexagonal

tessellation (hexagons with 500 m sides were used in Mission-Aransas National Estuarine Research Reserve and Corpus Christi Bay; hexagons with 750 m sides were used in the Upper and Lower Laguna Madre), was superimposed over all benthic areas characterized as >50% seagrass cover with a point randomly selected within each hexagon for annual monitoring and sampling.

Sampling was conducted within 10 m of the established GPS point. Field work occurred annually between mid-July and October in order to capture the period of peak seagrass biomass. Above-ground tissue samples were collected at every Tier-2 station where *H. wrightii* and/or *T. testudinum* were present. Five blades of each seagrass species present were haphazardly collected and measured to estimate canopy height. During sampling, instantaneous water quality measurements (temperature, depth, conductivity, salinity, and chlorophyll-*a*) were recorded using a YSI 6920 data sonde. Samples were kept on ice for transport back to the lab, where they were frozen until processing. While tissue samples were collected from each station at which seagrass was present, a spatially-representative subset of stations was selected for inclusion in this project in 2012 to reduce the volume of samples to be processed. In the following years (2013-2015) tissue samples were only processed from stations within this subset that historically had seagrass cover in order to allow for accurate, statistically robust interannual comparisons.

TISSUE ANALYSIS

Seagrass tissues were thawed, rinsed in Milli-Q ultrapure deionized water, and gently scraped using a clean scalpel to clear the tissue sample of debris, sediment, and epiphytes. Approximately 10 cm of blade tissue was subsectioned from the base of the photosynthetic region and the rest of the blade tissue was discarded. Plant root and rhizomes were not included in nutrient or isotopic analyses. Cleaned blade tissue samples were dried to a constant weight in an oven at 60ºC for approximately 4-7 days. When the tissue samples were fully dried, they were ground to a fine powder then stored at room temperature until elemental and isotopic analyses were conducted.

$\delta^{13}C$ and $\delta^{15}N$ and tissue C/N content analysis for 2013-2015 samples was conducted at the University of Texas Marine Science Institute using a Carlo Erba NC 2500 Elemental Analyzer interfaced through a Conflo II to a Finnigan MAT (Thermo) Delta Plus XL isotope ratio mass spectrometer. Samples collected during 2011 and 2012 were analyzed at the University of California, Davis Stable Isotope Facility using a PDZ Europa ANCA-GSL elemental analyzer interfaced to a PDZ Europa 20-20 isotope ratio mass spectrometer. Tissue P was quantified via a visible spectrophotometer using acid hydrolysis in conjunction with a colorimetric assay that produces a color reaction indicating total P content, according to modified methods of Chapman and Pratt (1961).

Stable isotope signatures are reported using the common $\delta^{A}X$ form, with A referring to an isotopic species of element X. The δ value is derived by comparing the isotope of interest to an established reference standard ($\delta^{A}X = (\frac{^{A}X_{sample}}{^{A}X_{STD}} - 1) * 1000$).

For C and N, these calculations compare a given sample's concentration of C-13 to the standard of PeeDee Belemnite (reported as $\delta^{13}C$) and N-15 to the standard of atmospheric N (reported as $\delta^{15}N$), respectively (Hayes 2004; Fry 2006).

GIS ANALYSIS

Preliminary statistical analysis was conducted using R 3.2.5 to determine if there were statistically significant differences in stoichiometric and isotopic signatures between *H. wrightii* and *T. testudinum* samples via a student's T-test. Based on these results (Table 3), further analyses were conducted separately for each species.

GIS analysis (ESRI ArcGIS ArcMap 10.3) was used to map spatial trends in isotopic and stoichiometric signatures and visualize changes in nutrient dynamics over time. Data points were divided into three spatial categories for analysis: Mission-Aransas Estuary/Corpus Christi Bay (MACC), Upper Laguna Madre (ULM), and Lower Laguna Madre (LLM), following the study design of Wilson and Dunton (2017).

All isoscape and stoichioscape maps were produced in ArcGIS ArcMap 10.3.1. Georeferenced isotopic and stoichiometric data were imported into ArcGIS and interpolated using an Ordinary Kriging method to assign a value to areas (cells) between sampling points. This interpolation methodology produces a smooth distance-dependent raster that was used to visualize spatial trends in $\delta^{13}C$ and $\delta^{15}N$ signatures and N:P ratios in each of the three regions from year to year. Cross validation tests were performed on each data subset (divided by parameter, year, and species) to compare three common methods of interpolation used for isoscape development in geospatial software: Inverse

Distance Weighting, Ordinary Kriging, and Empirical Bayesian Kriging. Cross validation tests and data visualizations were also performed to determine if a trend correction was required. Ideally, the method with the lowest root-mean-square error (RMSE) is used for interpolation as it produces the predicted values that are most closely aligned with observed values. For the majority of sampling groups, the most accurate model with the lowest RMSE was produced using an Ordinary Kriging interpolation with no trend correction and optimized model parameters. Ordinary Kriging interpolation often produces robust and accurate predictions of isotopic regimes and is commonly used to produce isoscapes in geoanalytical software, further supporting the use of this interpolation method for this analysis (del Castillo et al. 2013; Mallette et al. 2016; Pellegrini et al. 2016).

The model was optimized for all parameters, and default values were used for the other model conditions. The processing extent of the produced geoanalytical layer was extended to include the entirety of continuous seagrass cover as defined by the 2004/2007 NOAA Benthic Habitat Assessment and converted to a raster (using GA layer to grid tool). This raster was then clipped to the extent of continuous seagrass in the 2004/2007 Benthic Habitat Assessment and the color symbology was adjusted to reflect the same scale for all datasets.

The ArcGIS spatial statistics cluster and outlier analysis tool was used to identify regions of interest (i.e., localized $\delta^{13}C$ or $\delta^{15}N$ enrichment or depletion and N or P-limitation) by identifying statistically significant clusters of high and low values as well

as outlier values (for example, a low value present in a high value cluster) using the Anselin Local Moran's I statistic. This analysis assigns values a z-score that indicates relatively similarity or difference between stations compared to a random distribution of values. A highly positive score indicates statistically significant similarity between nearby stations (i.e., a cluster of either high or low values) while a highly negative score indicates statistically significant dissimilarity (i.e., the presence of a high value in a region of low values, or a low value in a region of high values). Clusters were considered significant if the p-value associated with their z-score was less than 0.05. Cluster analyses were conducted separately for each region and each year and included only stations where isotopic and elemental data was available (stations not included in the sampling subset were excluded from the statistical analysis).

STATISTICAL ANALYSIS

Statistical analyses were conducted in R Studio to identify significant variations in elemental and isotopic signatures between species and over time. Isotope and N:P data were checked for normality in order to confirm the appropriateness of ANOVA and regression analysis. In order to reduce the number of replicates in the analysis, data were grouped by region and comparisons were only made between stations where data were consistently collected over the five-year period. Repeated-measures ANOVA with Tukey post-hoc tests were used to test for differences in $\delta^{13}C$, $\delta^{15}N$, and N:P data within each region and within regions by year. Repeated measures ANOVAs only compared stations at which isotopic or stoichiometric data were available for all study years in order to

avoid biased statistical outcomes. Linear regression analysis was used to identify significant relationships between nutrient data and the environmental parameters of interest. Based on prior work, the environmental parameters considered were salinity, total suspended solids (TSS), chlorophyll-*a* concentration, depth, and DIN (NO_2^- + NO_3^-) or total N (TN).

In order to understand land-based human impacts, the isoscapes and stoichioscapes were overlain with the 2011 National Land Cover Database land use map and USGS HUC-10 watersheds. Distance regression analysis was used to determine if there were significant relationships between clusters of enriched or depleted isotope values or elevated N:P signatures and human development.

For the MACC, NOAA System-Wide Monitoring Program (SWMP) data collected in the Mission-Aransas National Estuarine Research Reserve was used in addition to environmental data collected as a part of Tier-2 monitoring. This data is collected on a monthly, weekly, or daily interval, providing a much finer resolution of analysis. Data was obtained from the National Estuarine Research Reserve System Centralized Data Management Office website (http://cdmo.baruch.sc.edu/). Data was used from the three Mission-Aransas NERR SWMP stations (Ship Channel, Aransas Bay, and Mesquite Bay) located within 10 km of at least three seagrass sampling stations. Water column nutrient data (NO_2^- + NO_3^- and chlorophyll-*a*) were collected monthly and salinity data were collected every 15 minutes. SWMP data were pooled by month to reflect conditions approximately 6-8 weeks prior to seagrass blade collection.

Consistently collected environmental data was available from the National Park Service (NPS) and Texas Commission for Environmental Quality (TCEQ) at four locations in the ULM and seven locations in the LLM. This data was pooled with seagrass sampling stations located within 5 km of the monitoring point (this was adjusted from 10 km in the MACC due to the proximity of monitoring points in the ULM and LLM). NPS data was collected continuously while TCEQ data was collected in duplicate samples once or twice a year. Like SMWP data, TCEQ and NPS data were pooled by month to reflect 6-8 weeks of environmental conditions prior to plant collection. This data was available for salinity, turbidity, TN, and chlorophyll-*a*.

Results

A summary of isotopic values ($\delta^{13}C$ and $\delta^{15}N$) and N:P ratios for *H. wrightii* and *T. testudinum* for the MACC, ULM, and LLM are reported in Tables 1 and 2 (*T. testudinum* is not found in the ULM). Isotopic and elemental values in *H. wrightii* tissues exhibited wide variation both spatially and temporally across all regions, though mean values for $\delta^{13}C$ and $\delta^{15}N$ from 2011-2015 fell close to the average $\delta^{13}C$ and $\delta^{15}N$ values reported in literature reviews by Kennedy et al. 2010 and Christiaen et al. 2014 summarizing studies of isotopic signatures of seagrasses. $\delta^{15}N$ and $\delta^{13}C$ signatures of *T. testudinum* blades were generally more enriched than isotopic signatures of *H. wrightii* blades in the MACC and LLM. Mean values for $\delta^{13}C$ and $\delta^{15}N$ signatures for *T. testudinum* again fell close to the average isotopic values reported in the same literature reviews of seagrass isotope studies (Kennedy et al. 2010, Christiaen et al. 2014, Fig. 2). Generally, $\delta^{15}N$, $\delta^{13}C$, and N:P values for *T. testudinum* blades were less variable than *H. wrightii* across all systems. $\delta^{13}C$ and $\delta^{15}N$ were negatively correlated for *H. wrightii* in the LLM ($r^2 = 0.27$), but not in *H. wrightii* in the MACC or ULM, or in *T. testudinum* (Fig. 13).

An initial student's T-test indicated that there were statistically significant differences between *H. wrightii* and *T. testudinum* samples (Table 3). All subsequent analyses were therefore conducted separately for the two species in each region.

ISOSCAPES AND STOICHIOSCAPE PATTERNS IN *H. WRIGHTII*

Cluster analysis revealed that each region exhibited distinct spatial trends in $\delta^{15}N$, $\delta^{13}C$, and N:P ratios that were significant and consistent across multiple years (significant p-values ranged from <0.0001 – 0.049; Table 8). Repeated measures ANOVAs and post-hoc tests indicated that *H. wrightii* $\delta^{13}C$ signatures were significantly different between all three regions (MACC-LLM p <0.0001, ULM-LLM p <0.0001, MACC-ULM p = 0.0002). Across the entire study area, $\delta^{13}C$ signatures significantly differed across years (p<0.001). There were also significant differences in $\delta^{15}N$ signatures between MACC and LLM (p=0.02) and ULM and LLM (p=0.01), but not between MACC and ULM (p = 0.99). There were significant differences in $\delta^{15}N$ within all three regions between years (p = 0.0007). *H. wrightii* N:P ratios varied significantly across all regions (MACC-LLM p <0.0001, ULM-LLM p <0.007, MACC-ULM p = <0.0001), and were much lower and less variable in the MACC than those of the ULM and LLM. N:P ratios all significantly varied within regions across years (p< 0.0001; Table 4). N:P ratios in all regions were particularly elevated in 2015, with max values of 61, 130, and 104 in the MACC, ULM, and LLM, respectively. Tukey post-hoc comparisons for interannual differences are reported in Table 9.

SPATIAL ANALYSIS – *H. WRIGHTII* IN THE MISSION ARANSAS NERR/CORPUS CHRISTI BAY (MACC)

In the MACC, *H. wrightii* $\delta^{13}C$ signatures ranged from -14.6 ‰ to -7.6 ‰ (std. dev = 1.1-1.6 ‰). $\delta^{13}C$ signatures generally exhibited a north-south enrichment gradient, with clusters of enriched values in Corpus Christi Bay and the southern part of Mission-

Aransas Estuary and depleted $\delta^{13}C$ clusters occurring in the northern parts of the Mission-Aransas Estuary. This trend is reversed in 2015. However, seagrass $\delta^{13}C$ signatures in 2015 across the entire MACC system were notably depleted compared to all previous years. This shift coincides with a large spring flooding event in May 2015 that resulted in an extended period of low salinity in the Mission-Aransas Estuary (Reyna et al. 2017; Fig. 3).

$\delta^{15}N$ signatures for the MACC ranged from -6.3 ‰ to 8.8 ‰ (std. dev = 1.6 - 2.7 ‰). Significant clusters of depleted $\delta^{15}N$ signatures occurred annually in the Redfish Bay region ($p < 0.0001 – 0.04$; Fig. 3). High (but not statistically significant) $\delta^{15}N$ signatures also occurred annually in Nueces Bay and Corpus Christi Bay. N:P ratios ranged from 13 to 61 (std. dev = 5.5-10.4). Cluster analysis indicated that in 2011 there were significant clusters of high N:P ratios in Corpus Christi Bay ($p < 0.0001 – 0.002$) and low N:P ratios in the Mission-Aransas estuary ($p = 0.0001 – 0.013$). This pattern was consistent in the following four years, but was much less apparent (Fig. 3). The majority of N:P values fell below 30, indicating that under normal conditions this is a N-limited system, though the average N:P ratio exceeded this threshold in 2015.

SPATIAL ANALYSIS – *H. WRIGHTII* IN THE UPPER LAGUNA MADRE (ULM)

In the ULM, $\delta^{15}N$, $\delta^{13}C$, and N:P values did not exhibit spatial patterns as strong as those seen in the MACC and LLM. There was also a high degree of variability across space and between years. $\delta^{13}C$ signatures in ULM ranged from -15.2 ‰ to -8.0 ‰ (std. dev = 1.3-1.5 ‰). A significant cluster of relatively depleted $\delta^{13}C$ signatures occurred in

2011, 2012, 2014, and 2015 in the north-central section of ULM ($p < 0.0001 – 0.03$; Fig. 4); though it was not statistically significant, a depleted $\delta^{13}C$ cluster also occurred in this region in 2013. A significant cluster of relatively high $\delta^{13}C$ signatures occurred in 2011, 2012, and 2015 (with a similarly high though not significant cluster occurring in 2013) in the area known as "Nine-Mile Hole," a notably shallow region of the ULM ($p < 0.0001 – 0.027$). This cluster was not associated with a notable area of development or agriculture.

$\delta^{15}N$ signatures in the ULM ranged from -6.2 ‰ to 5.8 ‰ (std. dev = 1.2-2.1 ‰). Though there was a large amount of variability in $\delta^{15}N$, values were fairly uniformly distributed across the ULM. Depleted $\delta^{15}N$ clusters occurred in 2012, 2013, 2014, and 2015 on the northeastern shore of the ULM ($p < 0.0001 – 0.04$). In 2011, 2012, 2013, and 2015 $\delta^{15}N$ signatures generally became more depleted from north to south; however, in 2014, this trend was reversed (Fig. 4).

H. wrightii N:P ratios in the ULM ranged from 12 to 130 (std. dev = 8-19). Average values consistently exceeded 30, indicated a generally P-limited system, with a notable upswing in 2015. In 2011 and 2015 clusters of significantly elevated N:P ratios occurred at the mouth of Baffin Bay ($p < 0.0001 – 0.02$), while in 2012, 2013, and 2014 clusters of elevated N:P ratios occurred along the eastern shore of the ULM ($p < 0.0001 – 0.03$; Fig. 4). Though the elevated clusters at the mouth of Baffin Bay may be associated with the drainage of Kingsville, TX, the eastern shore clusters are unassociated with human development or urbanization ($r^2 = 0.21$; Fig. 12).

SPATIAL ANALYSIS – *H. WRIGHTII* IN THE LOWER LAGUNA MADRE (LLM)

H. wrightii $\delta^{13}C$ signatures were relatively consistent throughout the LLM, ranging from -14.5 ‰ to -6.9 ‰ (std. dev = 1.2-1.5 ‰). However, significantly depleted $\delta^{13}C$ clusters occurred adjacent to the main outlet of the Arroyo Colorado in 2011 and 2013 and at an outlet of a branch north of the main Arroyo Colorado outlet in 2011 and 2014 ($p< 0.0001 – 0.01$; Fig. 5). These outlets both drain a watershed that is home to the urbanized towns of McAllen and Edinburg. This depleted cluster is significantly positively correlated with distance from the outlet, with $\delta^{13}C$ signatures increasing with distance from the outlet within 15 km ($r^2 = 0.37$; Fig. 12). A significant cluster of depleted $\delta^{13}C$ signatures also occurred annually in the northernmost point of seagrass extent in the LLM ($p <0.0001 – 0.04$). Unlike other clusters in the LLM, this is not associated with an area of development. Initially, during all five years of the study, a cluster of depleted $\delta^{13}C$ signatures was identified in the southernmost area of the LLM, in an area known as South Bay. However, this cluster was driven by a single data point collected in this area that was highly depleted relative to the other *H. wrightii* samples in the LLM. Upon removal of this outlier, a trend of decreasing $\delta^{13}C$ signatures from north-south remained in all years, though this trend was not significant (Fig. 5).

$\delta^{15}N$ signatures for the Lower Laguna Madre ranged from -4.3 ‰ to 9.8 ‰ (std. dev = 2.2-2.9 ‰) and N:P ratio values ranged from 18 to 104 (std. dev = 9-16). In the LLM, a consistent localized $\delta^{15}N$ enrichment ($p < 0.0001 - 0.04$) was present from 2011-2015 at the outlet of a tributary slightly north of the main branch of the Arroyo Colorado

(Fig. 5). This is the same outlet draining McAllen and Edinburgh that is similarly associated with localized $\delta^{13}C$ depletion (Fig. 12). Mirroring $\delta^{13}C$ trends, $\delta^{15}N$ signatures of seagrasses within 15 km of the Arroyo tributary mouth exhibited a negative linear relationship with distance from this outlet ($r^2 = 0.36$, Fig. 12). A cluster of significantly depleted $\delta^{15}N$ signatures appeared each year on the eastern side of the LLM basin ($p < 0.0001 – 0.04$; Fig. 5). Additionally, there was a general trend of $\delta^{15}N$ becoming more depleted from north to south. This north-south $\delta^{15}N$ depletion gradient was loosely negatively correlated with a north-south gradient in N:P ratios in the LLM ($r^2 = 0.19$; Fig. 5). This gradient indicates a north-south shift from P-limitation to N-limitation, though average values indicate a generally P-limited system. Unlike in the more developed MACC region, the elevated N:P ratios in the northern reaches of the LLM are not associated with large areas of development, urbanization, or land cultivation.

ENVIRONMENTAL ANALYSIS RESULTS – *H. WRIGHTII*

H. wrightii $\delta^{13}C$ signatures were not well correlated with TSS measurements in any region (MACC $r^2 = 0.02$, ULM $r^2 = 0.002$, LLM $r^2 = 0.02$; Table 5 and Fig. 14), though TSS had significant effects on $\delta^{13}C$ in the MACC ($p = 0.005$) and LLM ($p = 0.002$). Depth was negatively correlated with $\delta^{13}C$ in the ULM ($r^2 = 0.20$; Fig. 14-E), though it did not have a significant relationship with $\delta^{13}C$ in the MACC ($r^2 = 0.01$) or the LLM ($r^2 = 0.03$; Table 5 and Fig. 14). In the MACC, meanwhile, *H. wrightii* $\delta^{13}C$ signatures were negatively correlated with water column chlorophyll-*a* concentrations ($r^2 = 0.31$), but this relationship was not conserved in the ULM ($r^2 < 0.0001$) or the LLM (r^2

= 0.008; Table 5 and Fig. 16). Instantaneous sonde measurements of salinity collected through Tier-2 monitoring were not correlated with $\delta^{13}C$ in any region (MACC $r^2 = 0.004$, ULM $r^2 = 0.006$, LLM $r^2 = 0.008$; Table 5 and Fig. 17). However, when regularly collected or continuously logged, salinity data were pooled and compared to $\delta^{13}C$ signatures at seagrass sampling stations within 10 km of the collection point, MACC *H. wrightii* $\delta^{13}C$ signatures were correlated with salinity across all years ($r^2 = 0.32$; Fig. 6A). ULM $\delta^{13}C$ Pooled salinity had a significant effect on $\delta^{13}C$ signatures in the ULM ($p = 0.03$) but did explain a large amount of variation in $\delta^{13}C$ signatures ($r^2 = 0.12$), nor was there a significant relationship between pooled salinity and $\delta^{13}C$ in the LLM ($r^2 = 0.10$; Table 5 and Fig. 6B, C).

N:P ratios of *H. wrightii* tissues were consistently positively correlated with water column N; N:P ratios were correlated with DIN concentrations in the MACC ($r^2 = 0.42$; Fig 7), while N:P ratios were correlated with TN in the ULM and the LLM ($r^2 = 0.56$ and $r^2 = 0.36$; Fig. 7). N:P ratios in 2015 were significantly higher across all regions, particularly in the ULM.

There was a negative correlation between *H. wrightii* $\delta^{15}N$ signatures and N:P ratios in the LLM ($r^2 = 0.19$). This relationship was not present in the MACC ($r^2 = 0.04$) or in the ULM ($r^2 = 0.03$), though the eastern elevated clusters of N:P ratios in the ULM were located in the same region as the depleted $\delta^{15}N$ clusters (Fig. 7).

ISOSCAPE AND STOICHIOSCAPE PATTERNS IN *T. TESTUDINUM*

Generally, there were far fewer significant clusters in *T. testudinum* $\delta^{13}C$ and $\delta^{15}N$ isoscapes and N:P stoichioscapes than in *H. wrightii* (Table 10). Unlike in *H. wrightii* samples, $\delta^{13}C$ and $\delta^{15}N$ signatures in *T. testudinum* were rarely significantly correlated with development or land use patterns in the LLM. Repeated measures ANOVA tests indicated that $\delta^{13}C$ signatures were significantly different between the MACC and LLM ($p = 0.01$) and significantly varied across years ($p < 0.001$). $\delta^{15}N$ signatures also were not significantly different between the MACC and LLM ($p = 0.10$), but did vary significantly across years ($p = 0.03$), though this relationship was driven by only one significant pairwise comparison between 2013 and 2014. N:P ratios significantly differed between regions ($p < 0.0001$) and between years ($p < 0.0001$), though in the MACC this was driven by small-scale local variation (Table 6). Tukey post-hoc interannual pairwise correlations are in Table 11.

SPATIAL ANALYSIS – *T. TESTUDINUM* IN THE MISSION-ARANSAS NERR/CORPUS CHRISTI BAY (MACC)

T. testudinum $\delta^{13}C$ signatures in the MACC ranged from -13.5 ‰ to -7.0 ‰ (std. dev = 1.0-1.2 ‰). $\delta^{13}C$ signatures were significantly more depleted in 2015, though this shift was much more notable in the Mission-Aransas NERR than in Corpus Christi Bay. The 2015 shift in *T. testudinum* $\delta^{13}C$ signatures towards more depletion was not as dramatic as that seen in *H. wrightii* (Fig. 8).

$\delta^{15}N$ signatures for the MACC ranged from 0.5 ‰ to 7.1 ‰ (std. dev = 0.9 - 1.6 ‰). *T. testudinum* $\delta^{15}N$ was, on average, more enriched and exhibited a smaller range

than *H. wrightii* $\delta^{15}N$ in the MACC. In 2014, a significant high cluster occurred in southern Redfish Bay ($p < 0.0001 – 0.04$) and a significant low cluster occurred in northern Redfish Bay ($p = 0.03 – 0.04$). In 2015, a significant low cluster occurred in southwestern Redfish Bay ($p = 0.002 – 0.008$). The 2014 $\delta^{15}N$ enrichment in Redfish Bay coincided with a localized extreme enrichment in N:P ratios in Redfish Bay during the same year ($p < 0.0001 – 0.002$; Fig. 8). This elevated N:P ratio cluster was associated with distance from a wastewater treatment plant serving the relatively urbanized coastal towns of Aransas Pass ($r^2 = 0.21$ Fig. 12). *T. testudinum* N:P ratios were generally consistent across the region and reflected general N-limitation in 2012 and 2013 and P-limitation in 2011, 2014, and 2015, displaying a trend similar to that seen in *H. wrightii* in this region. N:P ratios ranged from 18 – 100 (std. dev = 3-20), though high values were driven by the 2014 extreme N:P enrichment in Redfish Bay (Fig. 8).

SPATIAL ANALYSIS – *T. TESTUDINUM* IN THE LOWER LAGUNA MADRE (LLM)

Unlike in *H. wrightii*, there were no discernible clusters in $\delta^{13}C$ and $\delta^{15}N$ signatures in *T. testudinum* at sites associated with human land use in the LLM. $\delta^{13}C$ signatures ranged from -11.8 ‰ to -6.2 ‰ (std. dev = 1.0 ‰ for all years). $\delta^{13}C$ signatures exhibited a slight north-south depletion gradient, but this trend was weaker than that observed in *H. wrightii*. *T. testudinum* $\delta^{13}C$ signatures were also less spatially variable across the entirety of the LLM than they were in *H. wrightii* (Fig. 9). Significantly low clusters of $\delta^{13}C$ occurred annually along the southeastern side of the LLM ($p < 0.001 – 0.038$) while significantly high clusters of $\delta^{13}C$ signatures occurred

annually along the southwestern side of the LLM ($p < 0.001 – 0.004$), though the range *T. testudinum* $\delta^{13}C$ signatures was narrower than that of *H. wrightii* and these clusters were not associated with areas of development or urbanization (Fig. 9).

$\delta^{15}N$ signatures in the Lower Laguna Madre ranged from -2.4 ‰ to 7.2 ‰ (std. dev = 1.3-1.9 ‰). Similar to the trend seen in the MACC, LLM *T. testudinum* $\delta^{15}N$ signatures were generally more enriched and exhibited a smaller range than those of *H. wrightii* (Fig. 9). A general pattern of enriched to depleted $\delta^{15}N$ signatures from north to south was present, but not statistically significant. Significant $\delta^{15}N$-depleted clusters were found on the southwestern side of the LLM ($p < 0.0001 – 0.02$), mirroring the trend seen in *H. wrightii* $\delta^{15}N$, and significant $\delta^{15}N$-enriched clusters occurred at the southernmost extent of continuous seagrass cover in the LLM ($p < 0.0001 – 0.04$). These elevated clusters are associated with the urbanized tourist hub of South Padre Island, though there was not a significant relationship between $\delta^{15}N$ and distance from the outlet draining these municipalities. These clustering patterns were consistent across all years.

N:P ratio values ranged from 20 to 88 (std. dev = 9-14; Table 2) and indicated general P-limitation, though N:P values exhibited a strong declining spatial gradient, indicating a shift from P-limitation in the northern LLM to N-limitation in the southern LLM and mirroring the trends seen in LLM *H. wrightii* (Fig. 9), though, again, this northern N:P enrichment does not appear to be associated with local human land use.

ENVIRONMENTAL ANALYSIS RESULTS – *T. TESTUDINUM*

In *T. testudinum* samples collected in the MACC and the LLM, there was not a relationship between $\delta^{13}C$ and depth (MACC $r^2 = 0.001$, LLM $r^2 = 0.001$; Fig. 16), or $\delta^{13}C$ and TSS (MACC $r^2 = 0.002$, LLM $r^2 = 0.02$; Fig. 16). *T. testudinum* $\delta^{13}C$ signatures were also not correlated with Tier-2 instantaneous salinity measurements, similar to the trend seen in *H. wrightii* tissues (MACC $r^2 = 0.03$, LLM $r^2 = 0.01$; Table 7 and Fig. 16), though instantaneous salinity did have a significant effect on $\delta^{13}C$ (MACC $p = 0.04$, LLM $p = 0.04$). However, again mirroring conditions in *H. wrightii*, when pooled *T. testudinum* $\delta^{13}C$ signatures were compared to pooled, regularly collected salinity data, there was a significant correlation in the MACC ($r^2 = 0.66$), though this relationship was not seen in the LLM ($r^2 = 0.004$; Fig. 10). *T. testudinum* $\delta^{13}C$ signatures were negatively correlated with chlorophyll-*a* concentrations in the MACC ($r^2 = 0.40$), but were positively correlated with chlorophyll-*a* concentrations in the LLM ($r^2 = 0.32$), contrasting all other regions (Fig. 17).

As observed with *H. wrightii* samples, LLM $\delta^{15}N$ and N:P ratios were loosely but significantly correlated (MACC $r^2 = 0.15$; LLM $r^2 = 0.13$; Fig. 11). However, in contrast with the distinct and consistent relationship between N:P ratios and water column N in *H. wrightii* tissues, N:P ratios in *T. testudinum* were neither significantly correlated with DIN in the MACC ($r^2 = 0.002$) nor with TN in the LLM ($r^2 = 0.05$; Fig. 11).

Discussion

Overall, isotopic and stoichiometric signatures for *T. testudinum* communities were less variable, more isotopically enriched, and characterized by lower N:P ratios than *H. wrightii* communities (Fig. 2). Previous studies of *H. wrightii* and *T. testudinum* in the Florida Keys have reported similar discrepancies between isotopic and stoichiometric signatures of the two species, with *T. testudinum* being more enriched in both $\delta^{13}C$ and $\delta^{15}N$ and *H. wrightii* exhibiting higher N:P ratios (Campbell and Fourqurean 2009).

There are some inherent differences in physiology and C and N assimilation between *H. wrightii* and *T. testudinum* that may account for the differences observed here. *H. wrightii* belongs to the Cymodoceaceae family, while *T. testudinum* belongs to the Hydrocharitaceae family, an evolutionary distinction that accounts for morphological, physiological, and functional differences between the species (Kuo and McComb 1998; Cook 1998). *H. wrightii* is a well-documented pioneer species, quickly colonizing and becoming established under a wide range of water quality conditions (Gallegos et al. 1994). It displays an aggressive guerilla growth and propagation strategy, through which it rapidly spreads into new environments. *T. testudinum*, meanwhile, is a climax species with a narrower range of optimal light, salinity, and oxygen conditions suitable for growth. *T. testudinum* engages in a phalanx strategy, growing at a slow rate with extensive branching (Dawes 1998; Touchette and Burkholder 2000). *T. testudinum* is adaptable to settlement in relatively nutrient-poor conditions, while *H. wrightii*'s rapid

colonizing growth strategy requires higher nutrient concentrations in the environment in which it settles (Fourqurean et al. 1995; Campbell and Fourqurean 2009). As a slower-growing and more robust plant with less benthic coverage than *H. wrightii*, the isotopic and stoichiometric signatures of *T. testudinum* also reflect a longer time scale and coarser spatial resolution, resulting in a "smoothing" of the isoscape and stoichioscape (i.e., the smaller range in values and spatial variation in *T. testudinum* iscoscapes and stoichioscapes in comparison with those of *H. wrightii*; Fig. 9 vs. Fig. 5).

Due to isotopic distinctions between bicarbonate (HCO_3^-) and CO_2, the assimilation and use of HCO_3^- results in $\delta^{13}C$ enrichment in seagrass tissues (Hemminga and Mateo 1996; Campbell and Fourqurean 2009). Both *H. wrightii* and *T. testudinum* are able to assimilate and utilize HCO_3^- as well as dissolved CO_2 to meet their C needs (Durako 1993). Though *H. wrightii* has been shown to have a higher affinity for HCO_3^- (Campbell and Fourqurean 2013), *T. testudinum* is more efficient at utilizing HCO_3^- (Durako 1993). Therefore, it is possible that on the Texas coast *T. testudinum* is assimilating HCO_3^- more effectively than *H. wrightii*, thus resulting in its generally higher $\delta^{13}C$ signatures.

Finally, the difference in isoscapes and stoichioscapes produced for *H. wrightii* and *T. testudinum* may be in part attributable to the methodology used to develop these maps. The Ordinary Kriging interpolation used a distance-weighting system to assign predicted values to each raster cell that does not have an exact measurement associated with it. Species distribution and seagrass cover fluctuated over the five-year period and

across the three regions, and the range of *T. testudinum* and *H. wrightii* presence varies based on a suite of habitat suitability factors. Because of this variation in the spatial and temporal distribution of our data points, the raster interpolations and the relative impact of each data point on the adjacent raster cells varies slightly for each year and between the two species. Though the chosen interpolation method resulted in the most accurate predicted values, these modeled values are influenced by the inherent patchiness of the raw data. The distributions of *T. testudinum* and *H. wrightii* across the Texas coast likely accounts for at least some of the discrepancies between the iscoscapes and stoichioscapes of these two species. Overall, the obviously distinct isoscapes and stoichioscapes produced by each species highlights important species-specific considerations that must be made when using isoscapes and stoichioscapes to define system characteristics.

ISCOSCAPE AND STOICHIOSCAPE REFLECTIONS OF ENVIRONMENTAL CONDITIONS

The importance of freshwater inputs to the coast was clearly illustrated in the 2015 shifts in $\delta^{13}C$ in both *H. wrightii* and *T. testudinum*. This was observed in the MACC, where $\delta^{13}C$ signatures appear to be governed by the source of the DIC pool. $\delta^{13}C$ signatures in MACC *H. wrightii* and *T. testudinum* were consistently more depleted than those in the ULM and LLM (Fig. 2) reflecting the importance of relatively depleted riverine DIC ($\delta^{13}C$ between 0 and -10 ‰) in the MACC, which is the endpoint for the Mission, Aransas, and Nueces Rivers (Diener 1975; Mooney and McClelland 2012). Following the significant spring storm flushing event in May 2015, $\delta^{13}C$ signatures in both species were significantly more depleted throughout the MACC compared to the

previous four years, likely reflecting an influx of terrestrially-derived C sources (Figs. 3 and 8). This is correlated with a sustained and substantial drop in salinity in the MACC following the May 2015 storm event, as reported by Reyna et al. (2017), which suggests an extended presence of riverine DIC (Fig. 6). The Laguna Madre in contrast is a hypersaline lagoon with extremely limited freshwater inputs (Onuf 2007). In the ULM and LLM salinities and DIC pools are much more stable over time due to limited riverine inputs, and thus the distinct temporal shift seen in $\delta^{13}C$ signatures in the MACC in 2015 was not apparent.

Similarly, this dataset reveals a distinct temporal shift in nutrient dynamics that occurred across the Texas coast in 2015. Both *H. wrightii* and *T. testudinum* datasets showed a distinct and significant increase in N:P ratios in all three regions (Figs. 3, 4, 5, 8, and 9). This increase may in part be due to the May 2015 flooding event, which ended a drought that had persisted in south Texas for three years (Texas Water Development Board 2017, Wilson and Dunton 2017). The flux of terrestrially-derived N into these systems during this storm event, after a long period of very limited inputs, may be responsible for this apparent shift in the nutrient regime of these systems (Reyna et al. 2017).

Based on previous work indicating that seagrass $\delta^{13}C$ signatures serve as a proxy for benthic light availability (Hu et al. 2012, McPherson et al. 2015), it was hypothesized that a significant negative relationship would be observed between declining $\delta^{13}C$ signatures and environmental factors that control water column light attenuation such as

increased depth or water column TSS. However, this relationship was not evident in either the MACC or LLM (Figs. 14 and 15). One possible explanation for this is that seagrasses in these systems do not contend with severe water column light attenuation. The MACC is a relatively shallow system with depths ranging from 6-130 cm and averaging 57 cm (Texas Seagrass Monitoring Program data). The LLM, while deeper on average than the MACC (range 10 – 185 cm, average 87 cm), is not a turbid system, so seagrasses in the LLM are usually not light-limited (Kowalski et al. 2009). The high irradiance environment in the LLM is reflected in the mean $\delta^{13}C$ signatures of both *H. wrightii* and *T. testudinum*, which are enriched in comparison to seagrasses in the MACC and ULM (Fig. 2).

In contrast, in the ULM, benthic light availability is much more variable due the greater range of depths (range 9 – 210 cm, average 84 cm) and variable water transparency. This variability makes light attenuation a relatively more important factor in the ULM, and a metric that can be detected in $\delta^{13}C$ tissue signatures. This was reflected in the negative relationship between decreasing *H. wrightii* $\delta^{13}C$ signatures with increasing depth (Fig. 14-E), with particularly notable clusters of enriched $\delta^{13}C$ in extremely shallow areas, such as Nine-Mile Hole.

A possible factor affecting light availability in this system not accounted for in this study is the interception of benthic light by seagrass epiphytes. Along with water column light attenuation by suspended solids, epiphytic attenuation can further reduce benthic light availability to seagrasses by up to 30% less than ambient photosynthetically

active radiation (PAR) (Brush and Nixon 2002; Kemp et al. 2004). Seagrasses on the Texas Gulf Coast are consistently moderately fouled by epiphytes (Texas Seagrass Monitoring program, unpublished data). Additionally, in a study conducted in 2008, seagrass epiphyte weights in the Corpus Christi Bay were significantly higher than that of seagrasses in the upper Laguna Madre (Gutierrez et al. 2010). Dunton (1990) similarly found that algal epiphytes play a dominant role in regulating light availability in the MACC. This regional differential in epiphyte prevalence can in part explain why in the MACC, where epiphytes are abundant, seagrass $\delta^{13}C$ signatures are unrelated to light attenuating parameters such as depth or TSS. This is supported by the correlation between decreasing $\delta^{13}C$ and chlorophyll-*a* concentrations (Figs. 15 and 17) in both species in the MACC, suggesting that light is being attenuated by intermediate photosynthesizes and demonstrating the importance of additional factors contributing to light attenuation on the upper coast.

In spite of regional and temporal variation in isotopic and stoichiometric regimes, some relationships were notably consistent. For instance, the positive correlation between tissue N:P ratios and water column N concentrations in *H. wrightii* is conserved across both time and space, appearing in all three regions and holding over the five years of this study (Fig. 7). This relationship would be expected; with higher N availability in the water column, N becomes less limiting for seagrasses, and the N:P ratio increases. The role of *H. wrightii* and *T. testudinum* as trackers of nutrient limitation has been well-documented in other systems (Campbell and Fourqurean 2009; Armitage et al. 2005;

Fourqurean et al. 1992). In this study, however, while *H. wrightii* N:P ratios vary significantly with N inputs on the Texas coast, *T. testudinum* does not appear to track N input with much accuracy (Figs. 7 and 11).

Across the Laguna Madre, seagrass N:P ratios displayed a general north-to-south gradient from P-limitation to N-limitation (i.e., N:P > 30 in the north and < 30 in the south). This trend is consistent across the ULM and LLM and over the five year study period (Figs. 5 and 9). Previous work has indicated that the LLM is a generally a N-limited system, while the ULM is P-limited and N replete (Kaldy and Dunton 2000; Dunton 1996; Herzka and Dunton 1997), which is supported by the seagrass N:P ratio trends observed here. One possible explanation for this is north-to-south variation in N availability is the change in sediment type along the Texas Gulf Coast on a latitudinal gradient; ULM sediments are sandy, with porewater ammonium concentrations exceeding 100 μM (Pulich 1985; Dunton 1994). In the LLM, sediments are terrigenous and comprised of fine sands and quartz, characteristics that are known to result in sediment N deficiencies (Brown et al. 1980; Short 1987), reflected in measured mean porewater ammonium concentrations of approximately 32 μM (Kowalski et al. 2009). Additionally, the Texas Coast exhibits a strong latitudinal gradient in freshwater inflows, with riverine inflow into the Laguna Madre becoming diminished in the south (Longley 1994). The limited opportunities for exchange in the LLM (with the exceptions of the Arroyo Colorado and Brownsville Ship Channel) may be in part responsible for the N-limitation seen in seagrasses in this region.

Significant localized $\delta^{15}N$ depletions were seen in both *H. wrightii* and *T. testudinum* in the MACC and LLM, with the lowest $\delta^{15}N$ signatures ranging across systems from -6.3 to -4.3. These highly depleted values may be related to N cycling by the microbial community, including ammonification and dissimilatory nitrate reduction to ammonium (DNRA), processes which result in depleted pools of reactive N (McCready et al. 1983; Möbius 2013; Nikolenko et al. 2018). DNRA in particular makes large contributions to N cycling in Texas coastal bays and the Laguna Madre (An and Gardner 2002; Gardner et al. 2006). These processes, along acquisition of isotopically depleted ammonium from the water column, may be responsible for the clusters of very depleted $\delta^{15}N$ seen in seagrasses in Redfish Bay, the ULM, and on the western side of the LLM (Figs. 3, 4 and 5).

Another consistently observed trend is the significant negative linear relationship between N:P ratios and $\delta^{15}N$ signatures in the MACC and LLM in both *H. wrightii* and *T. testudinum*. A similar relationship was reported in *T. testudinum* in Florida Bay by Fourqurean et al. (2005). Previous work has concluded that low N availability can result in reduced isotopic discrimination during N uptake by seagrasses (Campbell and Fourqurean 2009). With a larger available N pool, seagrasses preferentially take up N-14, resulting in more depleted $\delta^{15}N$ signatures in seagrass tissues, providing another possible explanation for the negative relationship seen here between seagrass N:P ratios and $\delta^{15}N$ signatures.

In the LLM, this relationship may also in part be explained by the presence of cyanobacterial mats at the land cut between the upper and lower Laguna Madre (Tunnell and Judd 2002). These cyanobacterial communities facilitate rapid and extensive N-fixation (Pulich and Rabalais 1986; Pulich and Scanlan 1987). The high N:P ratios in both *H. wrightii* and *T. testudinum* in the northern LLM indicate that N concentrations in the system are high in this region (Figs. 5 and 9). It appears that these inputs of N are being rapidly fixed by these cyanobacterial communities. N-fixation results in a slight depletion of the DIN pool (Unkovich 2013). The root-rhizome microhabitat of seagrass beds on the Texas Gulf coast are also known to support a robust community of N-fixing microbes (Welsh 2000; Brock 2001; Gardner et al. 2006). This process supplies a large amount of slightly δ^{15}N-depleted DIN required to maintain seagrasses' high levels of productivity. Additionally, these cyanobacterial mats may be partially responsible for the localized δ^{13}C depletions seen in the northern LLM, as their presence may impede light penetration and result in localized light limitation.

HUMAN LAND USE PATTERNS

Human land use is likely an important factor in seagrass isotopic and stoichiometric variation across the Texas coast. This dataset shows that localized significant depletions and enrichments in δ^{13}C, δ^{15}N, and N:P ratios in seagrass tissues are significantly correlated with distance from outfalls draining high population areas (Fig. 12). In particular, the influence of inputs from the Arroyo Colorado and Baffin Bay and cities such McAllen, Edinburg, Aransas Pass, and Kingsville were consistently

tracked through this dataset. Seagrass beds growing in close proximity to these urbanized areas were typified by clusters of enriched $\delta^{15}N$ signatures, depleted $\delta^{13}C$ signatures, or elevated N:P ratios that were significantly different from the isotopic and stoichiometric characteristics of seagrass meadows located further from areas of human influence. This was particularly notable in *H. wrightii* but also reflected in *T. testudinum*.

These relationships were most distinct in the LLM, where enriched $\delta^{15}N$ and depleted $\delta^{13}C$ signatures in *H. wrightii* were associated with a stream outlet draining the Arroyo Colorado watershed. This watershed is home to the relatively urbanized municipalities of McAllen and Edinburg (Fig. 12). N loading from the Arroyo Colorado was detected by a "plume" of enriched *H. wrightii* $\delta^{15}N$ signatures just north of the Arroyo Colorado, which flows through the municipalities of McAllen and Edinburg, entering the Laguna Madre. This N is then rapidly taken up by the nearshore seagrasses.

An N-inflow model developed by DeYoe et al. (2016) reported high concentrations of nitrate at flow gauges within the McAllen-Edinburg watershed in comparison with analogous data collected at other south Texas gauge stations. $\delta^{15}N$ signatures of the particulate N measured by DeYoe et al. (2016) at the McAllen-Edinburg flow gauge reflect the $\delta^{15}N$ signatures of *H. wrightii* blades collected from the "plume" cluster, indicating that anthropogenic N from the Arroyo watershed is likely responsible for enriched $\delta^{15}N$ signal in *H. wrightii*. Seagrass N:P ratios at this location however, while indicative of a N-replete system, were not significantly higher than the N:P ratios in seagrasses of surrounding beds. Therefore, while human-derived N appears to be

entering the Laguna Madre here, the excess N delivered to the system is likely undergoing rapid microbial processing.

Seagrasses in the LLM do not appear to be light-limited, although previous work has noted that there are localized exacerbations of turbidity due to sediment inputs associated with the Arroyo Colorado watershed (Kowalski et al. 2009). In this study, *H. wrightii* $\delta^{13}C$ tissue signatures in this region were significantly depleted within 20 km of the nearest outlet, providing evidence for localized light limitation on a small scale. Additionally, due to the proximity of this site to the mouth of the Arroyo Colorado, one of the only sources of freshwater to the LLM, it is likely that these localized clusters of depleted $\delta^{13}C$ in LLM seagrasses are also reflecting inputs of freshwater DIC.

Along with a localized $\delta^{13}C$ depletion at the Arroyo Colorado watershed, a distinct, though insignificant, C depletion pattern appeared in *H. wrightii* in the southernmost tip of the LLM, South Bay. This depletion was driven by one data point, as *H. wrightii* cover is sparse in the far south portions of the LLM. However, this area is similarly impacted by the development of the Brownsville watershed. It is unlikely that depleted $\delta^{13}C$ signatures in South Bay are the result of riverine DIC due to its close proximity to the point of exchange between the Laguna Madre and the Gulf of Mexico, so the available DIC pool would be expected to have a marine $\delta^{13}C$ signal (approximately 0 - 2 ‰).

These trends were not replicated in LLM *T. testudinum* isoscapes. A significant localized enrichment in *T. testudinum* $\delta^{15}N$ did occur consistently in South Bay, but there

was not a relationship between this cluster and distance from the Brownsville Ship Channel or other outfalls draining the area. The surrounding area includes Brownsville as well as the tourist hub of South Padre Island, and it is possible that this development is contributing in some way to the localized enrichment seen in this area.

In the MACC and the ULM, the relationship between development and seagrass nutrient dynamics is most strongly illustrated in the localized elevated N:P ratios seen in the Redfish Bay region in 2014 and at the mouth of Baffin Bay in 2015, respectively. These localized peaks were each significantly positively related to outfalls draining populated regions of the Texas coast, home to the towns of Aransas Pass and Rockport in the MACC and Kingsville in the ULM (Fig. 12). $\delta^{13}C$ and $\delta^{15}N$ patterns in the MACC did not exhibit any statistically significant relationships with development or urbanized areas, though enriched $\delta^{15}N$ clusters were observed in areas of high population and human activity, such as the Port of Corpus Christi and Redfish Bay (Figs. 3 and 8). It is possible that, due to the relatively high degree of urbanization and large variety of C and N inputs into the MACC region, isotopic signals of individual sources were undetectable in this dataset.

In the ULM, $\delta^{15}N$ and $\delta^{13}C$ distributions were not notably correlated with land use patterns. Much of the ULM is bordered by Padre Island National Seashore, a pristine and relatively unimpacted stretch of the lower Texas coast. This region's relatively pristine nature is reflected in isoscapes and stoichioscapes that represent the natural N and C cycling of the region. For example, the max $\delta^{15}N$ signatures in the ULM were

consistently lower than in both the MACC and the LLM, ranging from 4.05 to 5.8. These values are generally lower than what would be expected for anthropogenic N entering the system (McClelland et al. 1997).

In this study, *H. wrightii* tissues appear to be highly responsive to environmental perturbations, with a wide range of isotopic and stoichiometric signatures across both time and space. The sensitive isotopic response of *H. wrightii* to differentials in C or N inputs, as well as its close tracking of N inputs into the system (in both total N and DIN) make it a highly relevant bioindicator species for the Texas coast. *T. testudinum* appears less responsive to ephemeral or small-scale perturbations in nutrient regimes and factors impacting the DIC pool and light availability. However, the slow growth and assimilation of C and N in *T. testudinum* make this species an ideal indicator of long-term conditions within the system.

A significant co-varying relationship between $\delta^{13}C$ and $\delta^{15}N$ was observed in *H. wrightii* in the LLM (Fig. 13). This is a common trend seen in studies using isotopic markers to delineate trophic and ecological relationships but not common for organisms at the same trophic level, such as seagrasses. This covariance likely reflects anthropogenic effects on seagrass isotopic signatures in the LLM, which is home to large areas of pristine seagrasses as well as beds adjacent to centers of development that experience distinct localized impacts. N loading in concert with increases in turbidity and freshwater inputs result in depleted seagrass $\delta^{13}C$ signatures that reflect reduced light

availability and enriched $\delta^{15}N$ signatures that reflect the presence of human-derived N in the system.

CONCLUSIONS

Patterns in seagrass isotopic and stoichiometric ratios reveal distinct differences among geographic regions on the Texas coast with respect to the availability of light and inorganic N. Each region exhibits unique dynamics and a different suite of factors controlling nutrient and isotopic dynamics, highlighting the importance of system-conscious stable isotope studies. Land use also plays an important role in regulating the relative proportion of anthropogenic N that enters bays and lagoons based on variations in $\delta^{15}N$ signatures. These data also reveal key differences in the isotopic and elemental characteristics of *H. wrightii* and *T. testudinum*, which provide short and long term information on ecosystem condition, respectively.

I have shown that along the Texas coast, $\delta^{13}C$ and $\delta^{15}N$ signatures and N:P ratios in the dominant seagrass species are significantly related to areas of human land usage and development. I have also shown that isotopic and stoichiometric regimes in *H. wrightii* and *T. testudinum* reflect environmental regime shifts, including changes in DIC pools, light availability, and nutrient availability. Because of its responsiveness to environmental perturbations and anthropogenic impacts, *H. wrightii* is a useful and effective bioindicator species, though *T. testudinum* also responds to large-scale changes in environmental condition and N availability.

This study also demonstrates the importance of small-scale, localized impacts on coastal systems. My analysis did not reveal strong system-wide relationships between isotopic and stoichiometric relationships with most environmental parameters, but I did observe significant patterns in $\delta^{13}C$, $\delta^{15}N$, and N:P ratios in *H. wrightii* and *T. testudinum* on regional and sub-regional scales. In regions of relatively low urbanization and development, it is necessary to operate at smaller spatial and temporal scales to identify anthropogenic impacts. This is particularly important on the middle and lower Texas coast, a relatively pristine region that is currently experiencing rapid development.

This work also clearly shows the value of well-developed isoscapes and stoichioscapes informed by a large data set. Due to our extensive sampling, I was able to detect localized but important variations in seagrass nutrient status that would be imperceptible with a coarser scale of analysis. These results provide a foundation on which to build a stronger and more comprehensive program that provides local resource managers with appropriate tools to develop water quality criteria that affords improved protection to seagrass habitats.

Table 1. Summary of $\delta^{15}N$, $\delta^{13}C$, and N:P ratios in MACC, ULM, and LLM *H. wrightii* blade tissue.

Region	Year	Mean $\delta^{15}N$	Std. Dev. $\delta^{15}N$	Min $\delta^{15}N$	Max $\delta^{15}N$	Mean $\delta^{13}C$	Std. Dev. $\delta^{13}C$	Min $\delta^{13}C$	Max $\delta^{13}C$	Mean NP	Std. Dev. NP	Min NP	Max NP
MACC	2011	1.5	1.6	-5.1	6.9	-10.4	1.2	-13.67	-8.3	30	5.8	19	47
	2012	1.7	2.1	-4.6	7.4	-10.6	1.6	-16.5	-8.1	25	6.3	13	43
	2013	2.2	1.7	-0.9	7.6	-10.3	1.4	-13.8	-8.1	26	5.5	14	40
	2014	2.0	1.9	-4.1	8.8	-10.5	1.1	-13.2	-7.6	30	9.5	13	49
	2015	1.0	2.7	-6.3	7.4	-11.9	1.3	-14.6	-9.6	34	10.4	15	61
ULM	2011	1.3	1.4	-2.8	5.3	-11.3	1.5	-14.8	-8.1	44	9.6	19	72
	2012	2.6	1.3	-0.8	4.4	-10.4	1.3	-13.6	-8.2	34	8.9	14	59
	2013	2.1	1.2	-0.9	5.5	-11.2	1.3	-13.6	-8.0	33	8.3	14	54
	2014	1.5	2.0	-5.3	4.0	-11.9	1.4	-15.5	-9.0	39	10.8	12	62
	2015	1.7	2.1	-6.2	5.8	-11.4	1.5	-14.5	-8.4	64	18.9	34	130
LLM	2011	1.4	2.4	-3.8	7.3	-9.6	1.3	-13.1	-6.9	45	10.8	22	74
	2012	3.0	2.2	-1.6	8.1	-9.0	1.2	-12.7	-7.2	33	9.0	18	57
	2013	3.1	2.2	-2.0	8.2	-9.4	1.3	-14.5	-7.2	43	11.2	22	66
	2014	3.4	2.3	-1.8	9.8	-9.9	1.5	-14.2	-7.3	49	14.8	26	80
	2015	2.4	2.9	-4.3	9.2	-9.7	1.4	-13.6	-7.2	56	15.8	22	104

Table 2. Summary of $\delta^{15}N$, $\delta^{13}C$, and N:P ratios in MACC and LLM *T. testudinum* blade tissue.

Region	Year	Mean $\delta^{15}N$	Std. Dev. $\delta^{15}N$	Min $\delta^{15}N$	Max $\delta^{15}N$	Mean $\delta^{13}C$	Std. Dev. $\delta^{13}C$	Min $\delta^{13}C$	Max $\delta^{13}C$	Mean NP	Std. Dev. NP	Min NP	Max NP
MACC	2011	3.2	1.3	1.0	6.4	-8.6	1.2	-13.5	-7.0	34	5	26	45
	2012	3.4	1.0	1.2	5.4	-9.0	1.1	-11.3	-7.5	28	3	22	34
	2013	3.8	1.0	0.5	6.0	-8.7	1.0	-12.7	-7.1	26	5	18	44
	2014	3.0	1.6	1.1	7.1	-9.0	1.0	-11.6	-7.0	38	20	20	100
	2015	3.8	0.9	1.7	5.9	-10.1	1.1	-13.5	-8.1	33	8	19	50
LLM	2011	2.7	1.9	-2.4	6.5	-8.5	1.0	-11.3	-6.7	36	10	20	62
	2012	2.8	1.4	0.2	5.6	-8.5	1.0	-10.6	-6.3	36	11	23	88
	2013	3.1	1.6	0.1	6.3	-8.6	1.0	-10.6	-6.2	39	9	23	67
	2014	2.8	1.3	0.5	5.8	-9.0	1.0	-11.8	-6.9	42	14	23	83
	2015	3.2	1.7	-1.1	7.2	-8.6	1.0	-11.8	-6.4	43	12	26	83

Table 3. Pairwise comparison of isotopic signatures of *H. wrightii* and *T. testudinum* tissues at the same station in the same year. Significant relationship are denoted by an asterisk (*).

	μ *H. wrightii*	μ *T. testudinum*	p-value
$\delta^{13}C$	-9.497	-8.583	<0.001*
$\delta^{15}N$	1.803	3.114	<0.001*

Table 4. Repeated measures ANOVA and interregional Tukey post-hoc test results, *H. wrightii.* Significant relationship are denoted by an asterisk (*). S.E. is standard error. Tukey post-hoc tests for interannual variation within regions are in Table 9 (appendix).

$\delta^{13}C$ Repeated Measures ANOVA				
	F	**D.f.**	**p-value**	
Region	74.367	2	<0.0001*	
Year	48.228	1	<0.0001*	
Region*Year	5.453	2	0.004*	
Tukey Post-Hoc Tests				
	Estimate	**S.E.**	**z-value**	**p-value**
MACC – LLM	-1.1277	0.1533	-7.354	<0.001*
MACC – ULM	-0.639	0.1584	-4.033	0.001*
ULM – LLM	-1.7668	0.145	-12.185	<0.001*
$\delta^{15}N$ Repeated Measures ANOVA				
	F	**D.f.**	**p-value**	
Region	3.6552	2	0.03*	
Year	11.6099	1	0.0007*	
Region*Year	9.3232	2	<0.0001*	
Tukey Post-Hoc Tests				
	Estimate	**S.E.**	**z-value**	**p-value**
MACC – LLM	-0.62077	0.23844	-2.603	0.02*
MACC – ULM	-0.03248	0.22519	-0.132	0.99
ULM – LLM	-0.65326	0.24639	-2.901	0.01*
N:P Repeated Measures ANOVA				
	F	**D.f.**	**p-value**	
Region	114.7759	2	<0.0001*	
Year	89.3092	1	<0.0001*	
Region*Year	6.0716	2	0.002*	
Tukey Post-Hoc Tests				
	Estimate	**S.E.**	**z-value**	**p-value**
MACC – LLM	-17.167	1.156	-14.856	<0.001*
MACC – ULM	13.846	1.193	11.603	<0.001*
ULM – LLM	-3.321	1.095	-3.032	0.007*

Table 5. Results of linear regression analysis of $\delta^{13}C$, $\delta^{15}N$, and N:P ratios with relevant environmental parameters, *H. wrightii*. Significant relationships are starred. Instantaneous salinity measurements were collected concurrently with plant samples during Texas Seagrass Monitoring program Tier-2 annual survey. Pooled salinity data was collected from regularly-visited SWMP, NPS, or TCEQ stations and pooled by month with the data from the closest seagrass monitoring stations. Significant relationships are denoted with an asterisk (*).

H. wrightii	**Relationship**	**r^2 value**	**p-value**
MACC	$\delta^{13}C$ vs. TSS*	0.02	0.005
	$\delta^{13}C$ vs. Chl- *a* *	0.31	0.03
	$\delta^{13}C$ vs. Instantaneous salinity	0.004	0.25
	$\delta^{13}C$ vs. Pooled salinity *	0.32	0.03
	$\delta^{13}C$ vs. Depth	0.01	0.05
	N:P ratio vs. DIN *	0.42	0.008
	$\delta^{15}N$ vs. N:P ratio	0.04	0.0007
ULM	$\delta^{13}C$ vs. TSS	0.002	0.46
	$\delta^{13}C$ vs. Chl- *a*	<0.0001	0.99
	$\delta^{13}C$ vs. Instantaneous salinity	0.006	0.15
	$\delta^{13}C$ vs. Pooled salinity *	0.12	0.03
	$\delta^{13}C$ vs. Depth *	0.20	<0.0001
	N:P ratio vs. TN *	0.56	0.02
	$\delta^{15}N$ vs. N:P ratio *	0.03	0.0005
LLM	$\delta^{13}C$ vs. TSS*	0.02	0.002
	$\delta^{13}C$ vs. Chl- *a*	0.008	0.56
	$\delta^{13}C$ vs. Instantaneous salinity	0.008	0.06
	$\delta^{13}C$ vs. Pooled salinity	0.10	0.30
	$\delta^{13}C$ vs. Depth	0.03	<0.0001
	N:P ratio vs. TN *	0.36	0.02
	$\delta^{15}N$ vs. N:P ratio *	0.19	<0.0001

Table 6. Repeated measures ANOVA test results, *T. testudinum* (post-hoc not required). Significant relationship are denoted by an asterisk (*).Tukey post-hoc tests for interannual variation within regions are in Table 11 (appendix).

$\delta^{13}C$ Repeated Measures ANOVA			
	F	**D.f.**	**p-value**
Region	6.4078	1	0.01*
Year	23.0968	1	<0.0001*
Region*Year	11.2225	1	0.0009*
$\delta^{15}N$ Repeated Measures ANOVA			
	F	**D.f.**	**p-value**
Region	2.7026	1	0.10
Year	4.9069	1	0.03*
Region*Year	0.0014	1	0.97
N:P Repeated Measures ANOVA			
	F	**D.f.**	**p-value**
Region	16.6177	1	<0.0001*
Year	31.0813	1	<0.0001*
Region*Year	4.2115	1	0.04*

Table 7. Results of linear regression analysis of $\delta^{13}C$, $\delta^{15}N$, and N:P ratios with relevant environmental parameters, *T. testudinum*. Significant relationships are starred. Instantaneous salinity measurements were collected concurrently with plant samples during Texas Seagrass Monitoring program Tier-2 annual survey. Pooled salinity data was collected from regularly-visited SWMP or TCEQ stations and pooled by month with the data from the closest seagrass monitoring stations. Significant relationships are denoted with an asterisk (*).

T. testudinum	**Relationship**	**r^2 value**	**p-value**
MACC	$\delta^{13}C$ vs. TSS	0.002	0.62
	$\delta^{13}C$ vs. Chl- *a* *	0.40	0.05
	$\delta^{13}C$ vs. Instantaneous salinity*	0.03	0.04
	$\delta^{13}C$ vs. Pooled salinity *	0.66	0.004
	$\delta^{13}C$ vs. Depth	0.001	0.67
	N:P ratio vs. DIN	0.002	0.89
	$\delta^{15}N$ vs. N:P ratio*	0.15	<0.0001
LLM	$\delta^{13}C$ vs. TSS*	0.02	0.01
	$\delta^{13}C$ vs. Chl- a *	0.32	0.009
	$\delta^{13}C$ vs. Instantaneous salinity*	0.01	0.04
	$\delta^{13}C$ vs. Pooled salinity	0.004	0.81
	$\delta^{13}C$ vs. Depth	0.001	0.50
	N:P ratio vs. TN	0.05	0.44
	$\delta^{15}N$ vs. N:P ratio *	0.13	<0.0001

Figure 1. Tier 2 sampling stations, Mission-Aransas Estuary and Corpus Christi Bay (MACC), Upper Laguna Made (ULM), and Lower Laguna Madre (LLM).

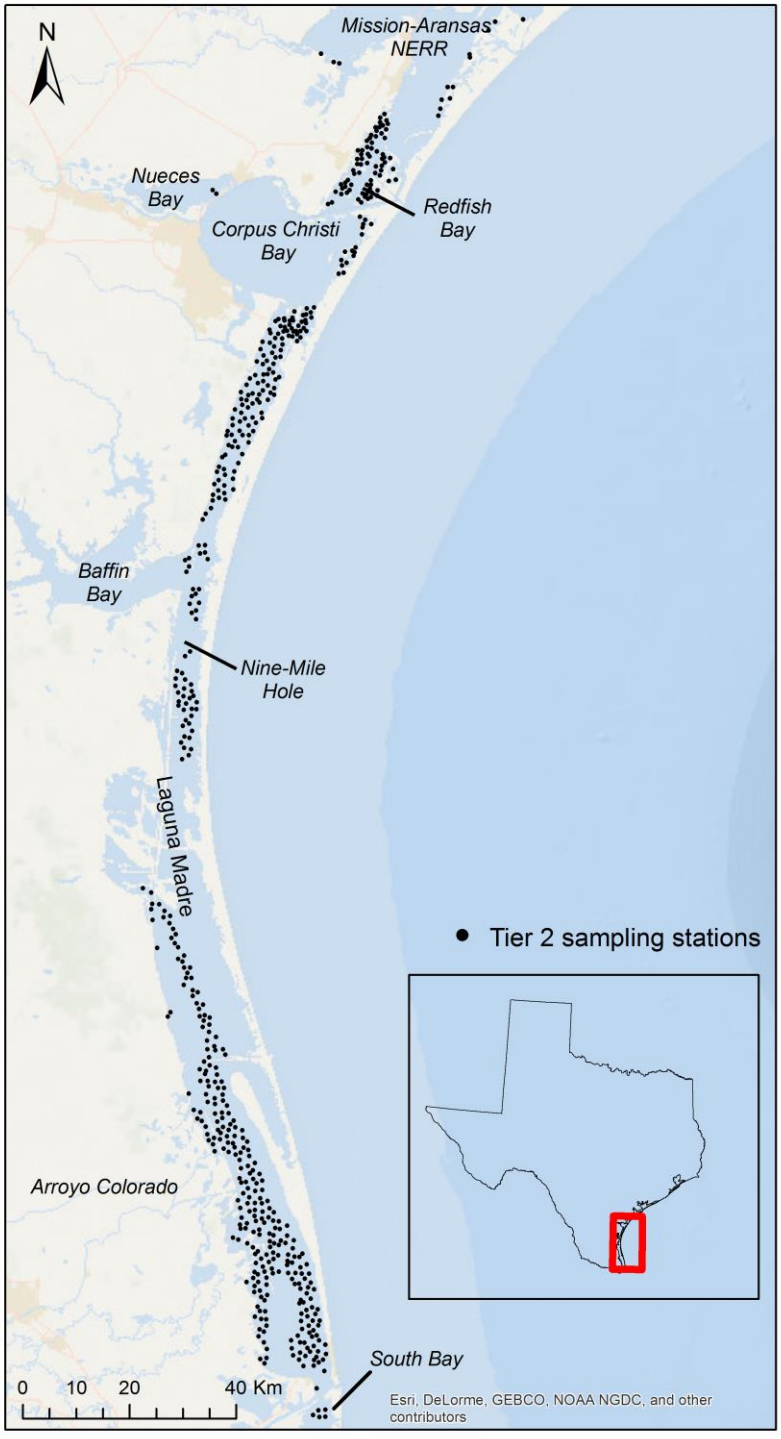

Figure 2. Mean *H. wrightii* and *T. testudinum* (a, d) $\delta^{13}C$ signatures, (b, e) $\delta^{15}N$ signatures, and (c, f) N:P ratios tissues in MACC, ULM and LLM, 2011-2015. Grey bars are standard error. Orange line indicates inflection point between N-limitation (N:P < 30) and P-limitation (N:P > 30). Pairwise statistical relationships are shown in Tables 8 and 9 (appendix).

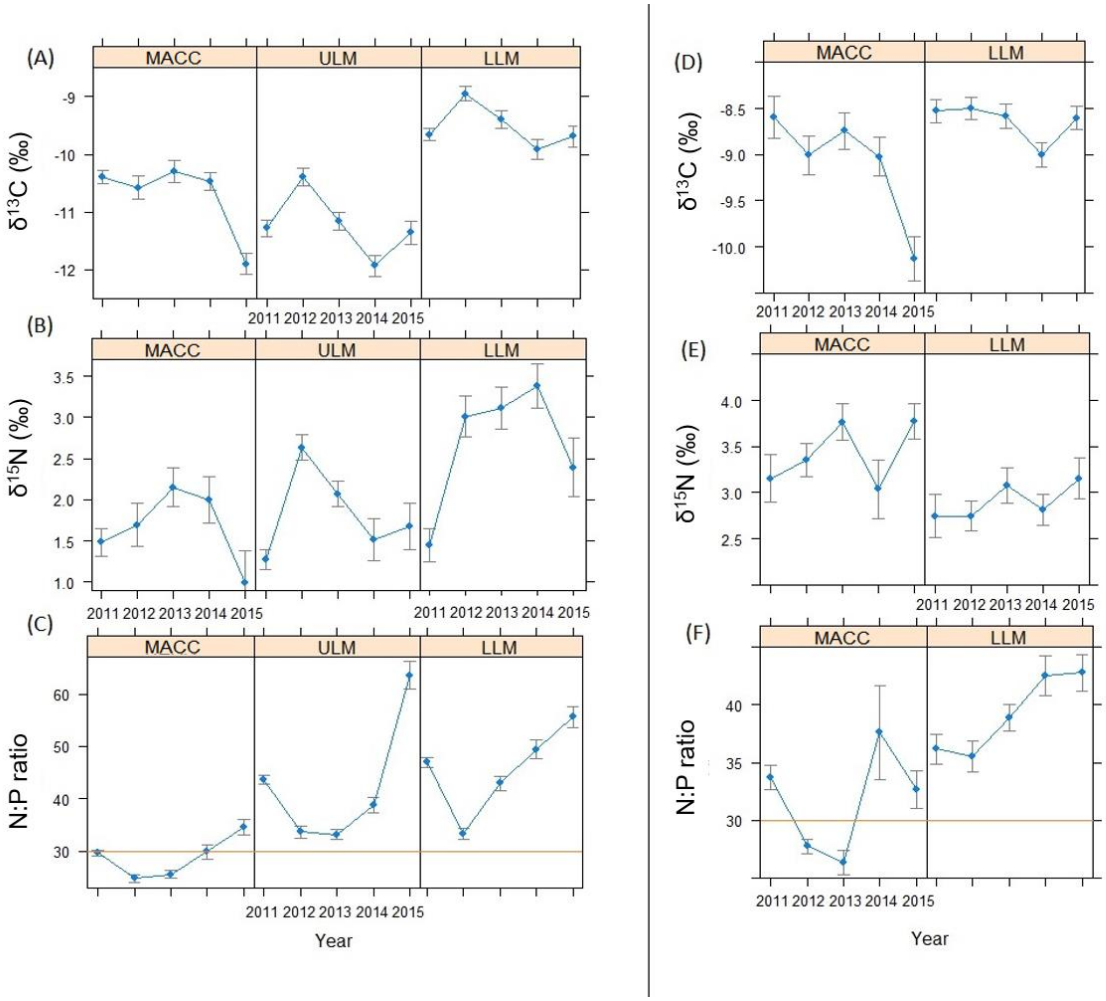

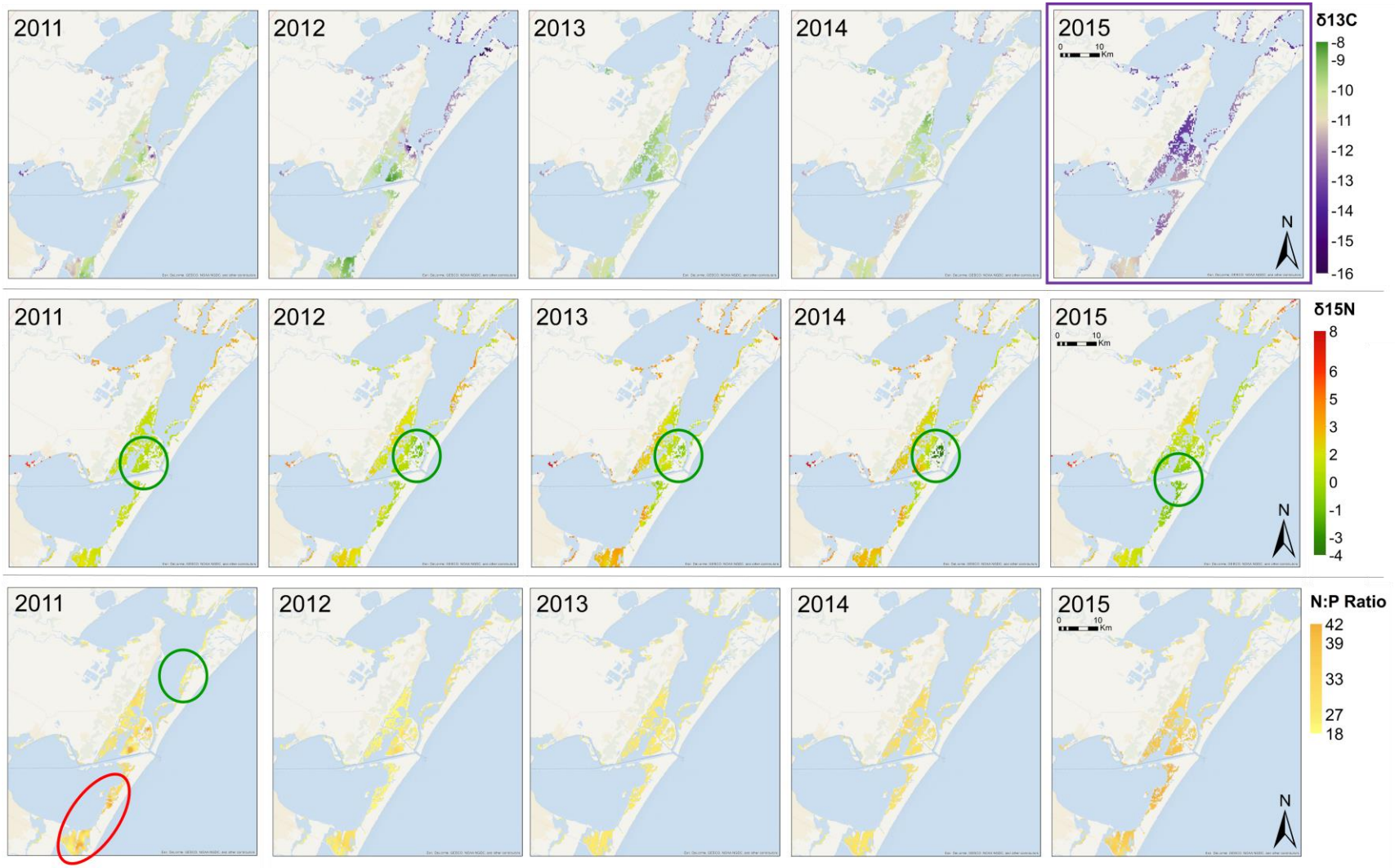
2011
2012
2013
2014
2015
0 10 Km
N
δ13C
-8
-9
-10
-11
-12
-13
-14
-15
-16
δ15N
8
6
5
3
2
0
-1
-3
-4
N:P Ratio
42
39
33
27
18

Figure 3.

Figure 3. Isoscapes and stoichioscapes of *H. wrightii* in the MACC, 2011-2015. Top: $\delta^{13}C$ signatures. Middle: $\delta^{15}N$ signatures. Bottom: N:P ratios. Green circles denote significant clusters of low values, red circles denote significant clusters of high values ($p < 0.05$). Purple box highlights significant shift in $\delta^{13}C$ following 2015 storm event.

Figure 4. Isoscapes and stoichioscapes of *H. wrightii* in the ULM, 2011-2015. Top: $\delta^{13}C$ signatures. Middle: $\delta^{15}N$ signatures. Bottom: N:P ratios. Green circles denote statistically significant clusters of low values, red circles denote statistically significant clusters of high values ($p < 0.05$).

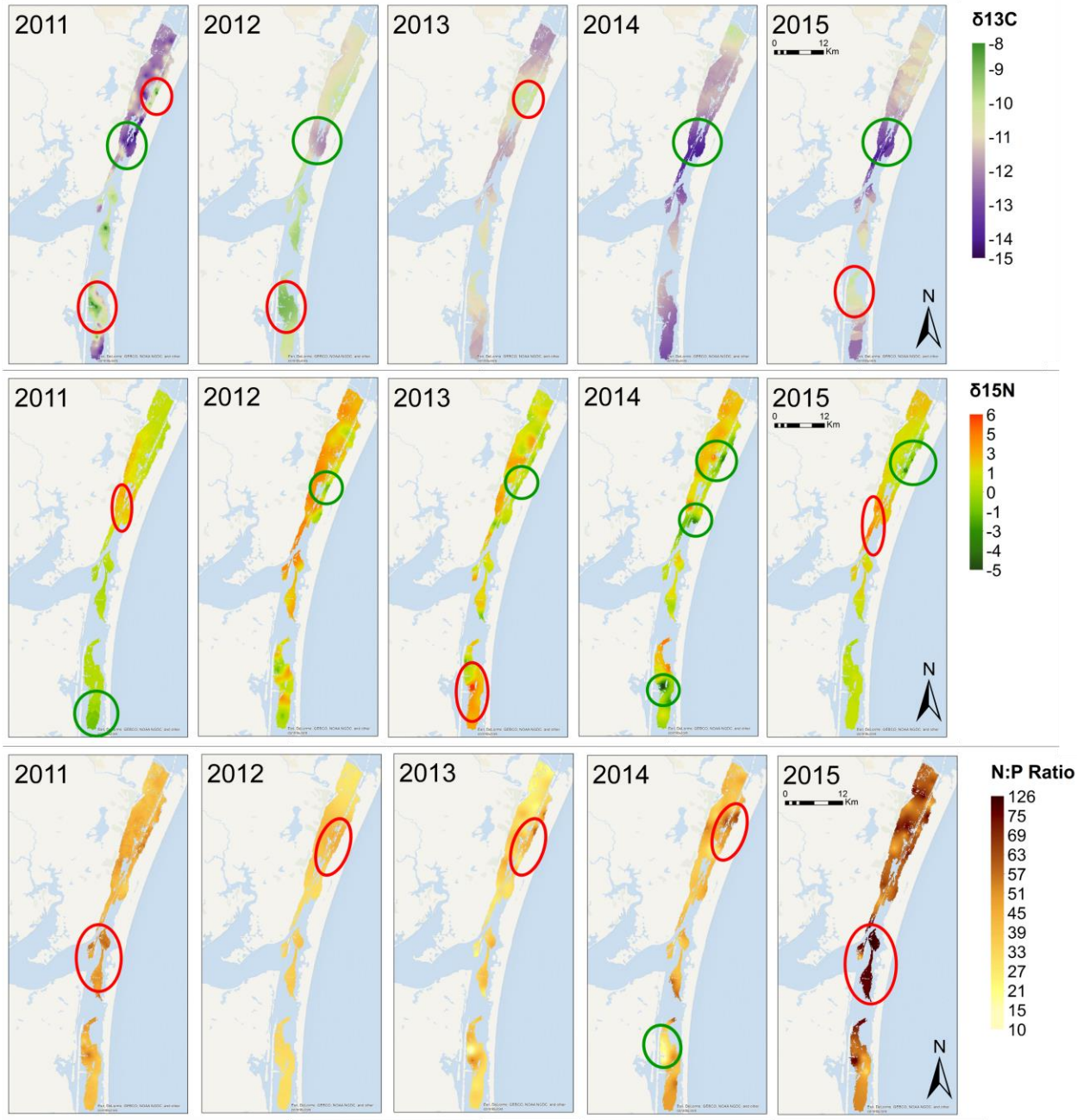

Figure 5. Isoscapes and stoichioscapes of *H. wrightii* in the LLM, 2011-2015. Top: $\delta^{13}C$ signatures. Middle: $\delta^{15}N$ signatures. Bottom: N:P ratios. Green circles denote statistically significant clusters of low values, red circles denote statistically significant clusters of high values ($p < 0.05$).

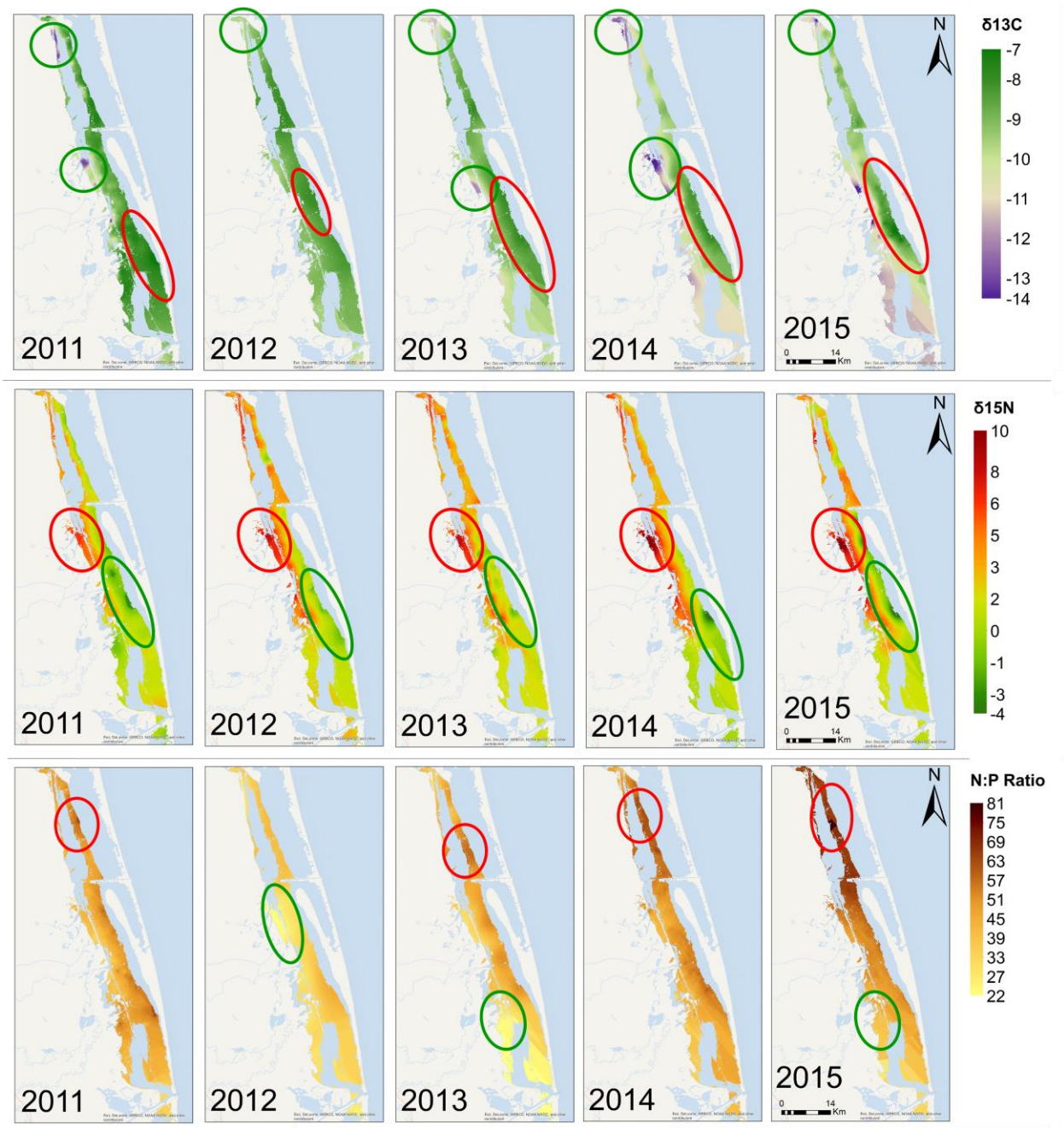

Figure 6. Pooled salinity readings collected during regular environmental monitoring 6-8 weeks prior to plant tissue collection vs. pooled *H. wrightii* $\delta^{13}C$ signatures at stations within 10 km (MACC) or 5 km (ULM/LLM), in (a) MACC, (b) ULM, and (c) LLM, 2011-2015.

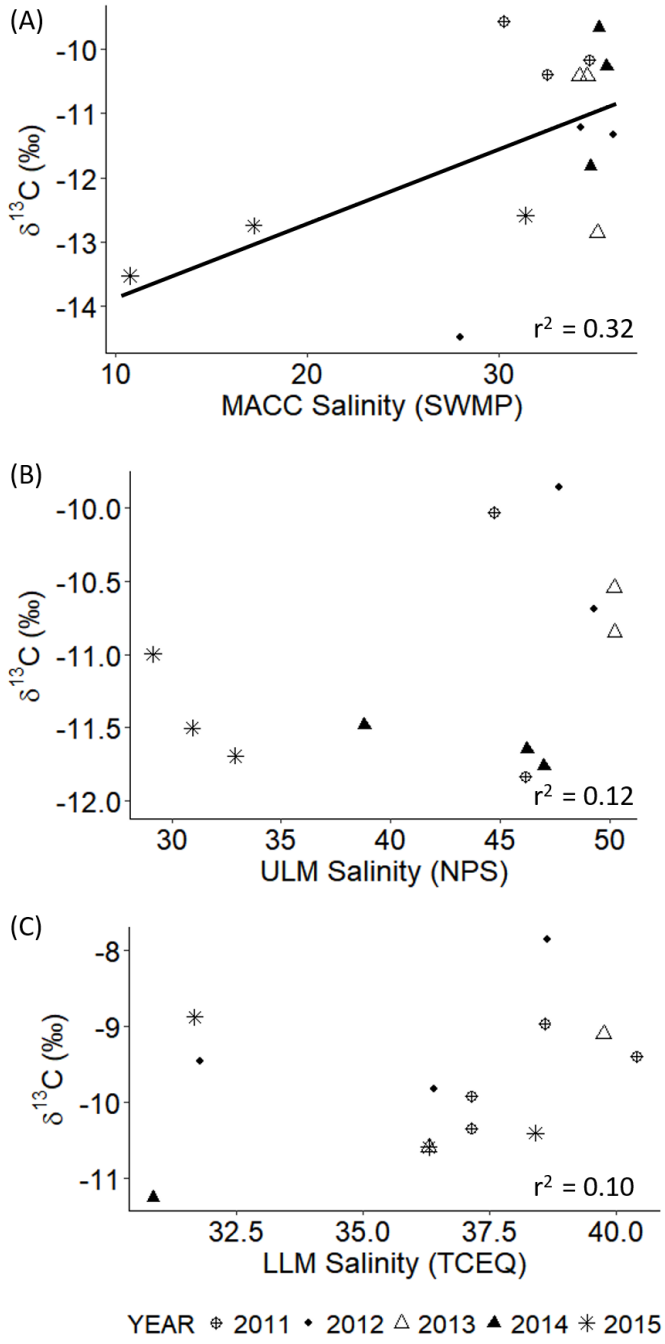

Figure. 7. Pooled water column N concentrations in (DIN SMWP data in the MACC), TN NPS/TCEQ data in the ULM and LLM) measured during regular environmental monitoring 6-8 weeks prior to plant tissue collection vs. pooled *H. wrightii* N:P ratios at stations within 10 km (MACC) or 5 km (ULM/LLM), in (a) MACC, (b) ULM, and (c) LLM from 2011-2015. $\delta^{15}N$ relationship with N:P ratios in (d) MACC, (e) ULM and (f) LLM.

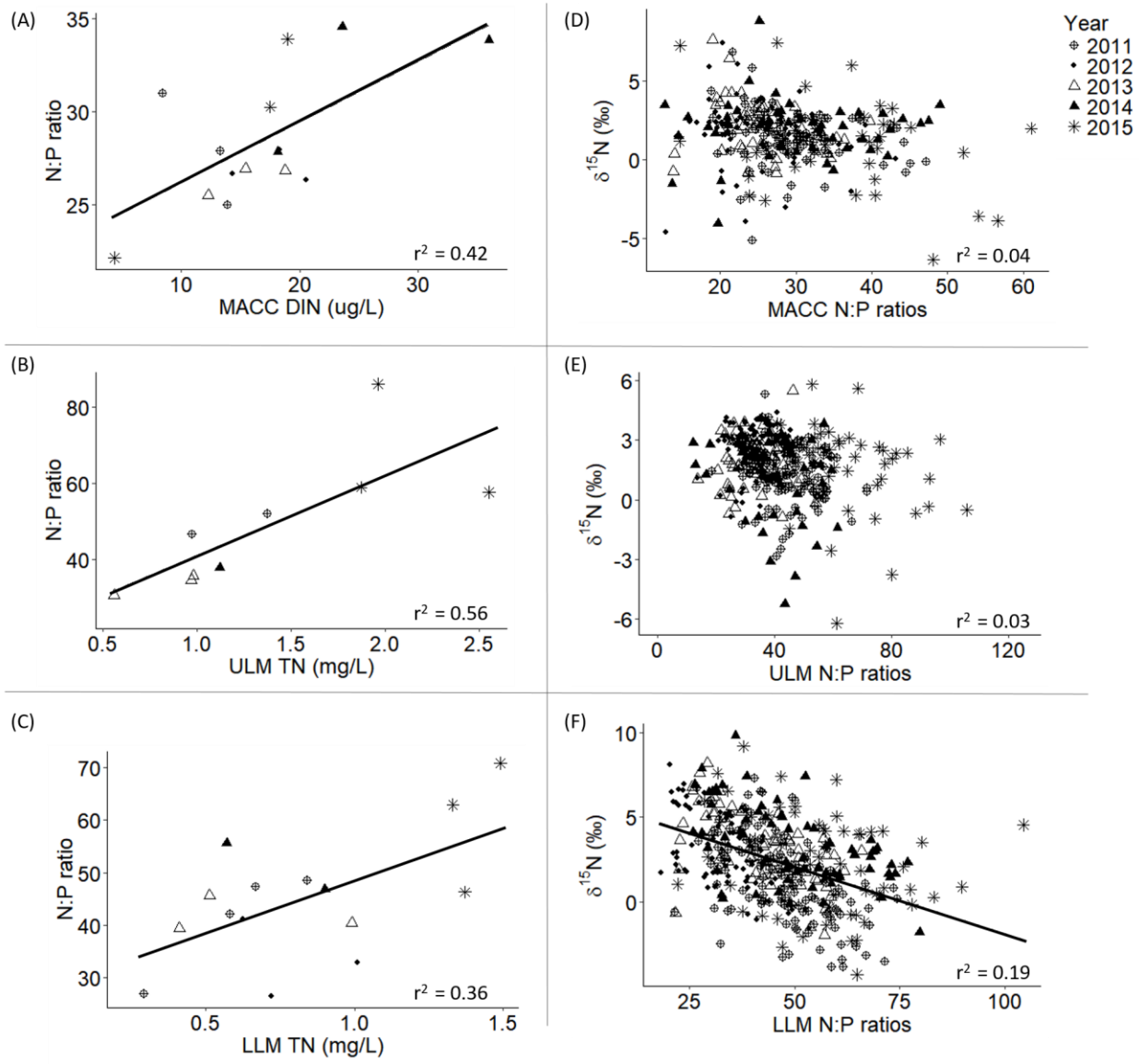

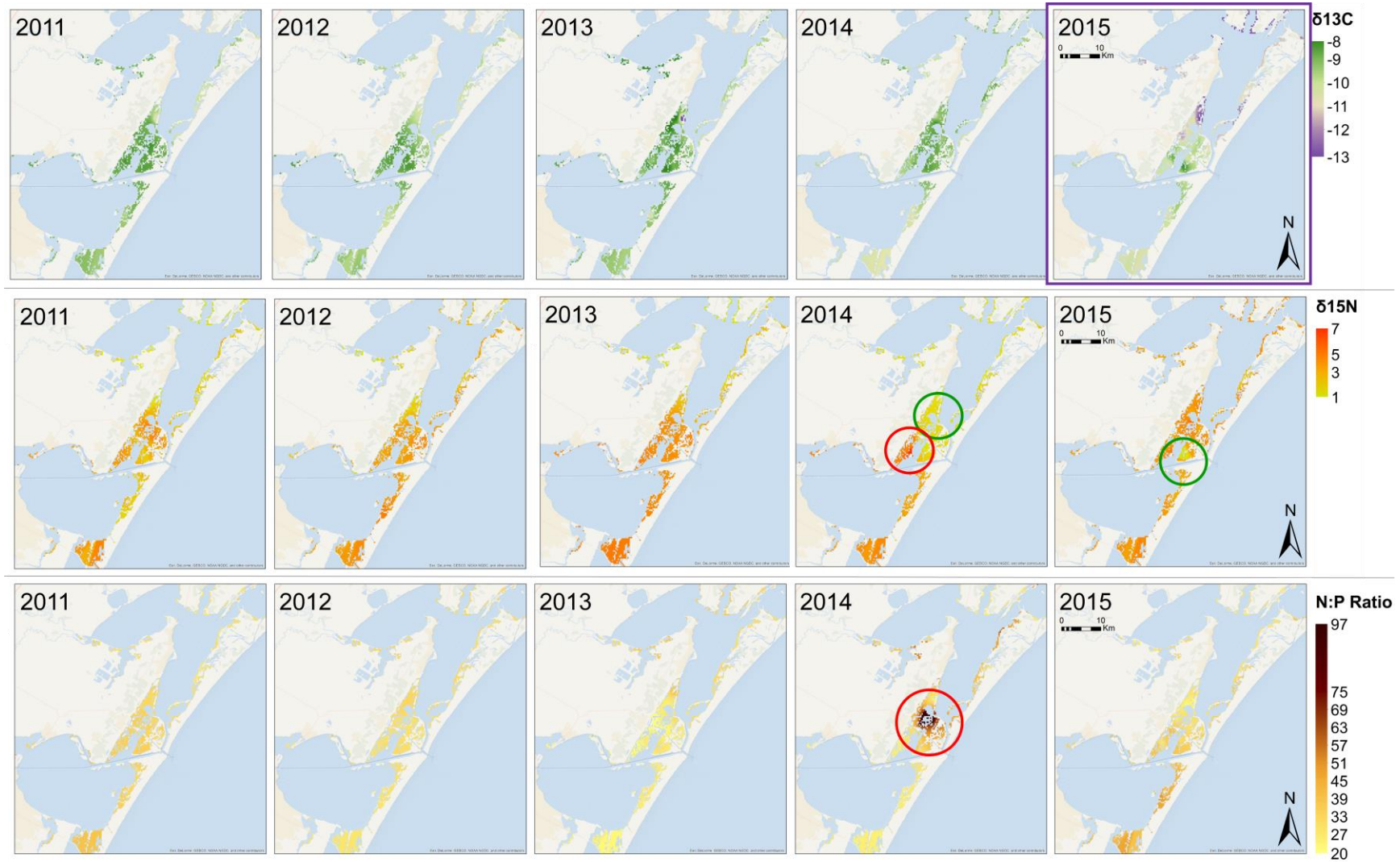
2011
2012
2013
2014
2015
0 10 Km
N
δ13C
-8
-9
-10
-11
-12
-13
δ15N
7
5
3
1
N:P Ratio
97
75
69
63
57
51
45
39
33
27
20

Figure 8.

Figure 8. Isoscapes and stoichioscapes of *T. testudinum* in the MACC, 2011-2015. Top: $\delta^{13}C$ signatures. Middle: $\delta^{15}N$ signatures. Bottom: N:P ratios. Green circles denote statistically significant clusters of low values, red circles denote statistically significant clusters of high values ($p < 0.05$). Purple box highlights significant shift in $\delta^{13}C$ following 2015 storm event.

Figure 9. Isoscapes and stoichioscapes of *T. testudinum* in the LLM, 2011-2015. Top: $\delta^{13}C$ signatures. Middle: $\delta^{15}N$ signatures. Bottom: N:P ratios. Blue/green circles denote statistically significant clusters of low values, red circles denote statistically significant clusters of high values ($p < 0.05$).

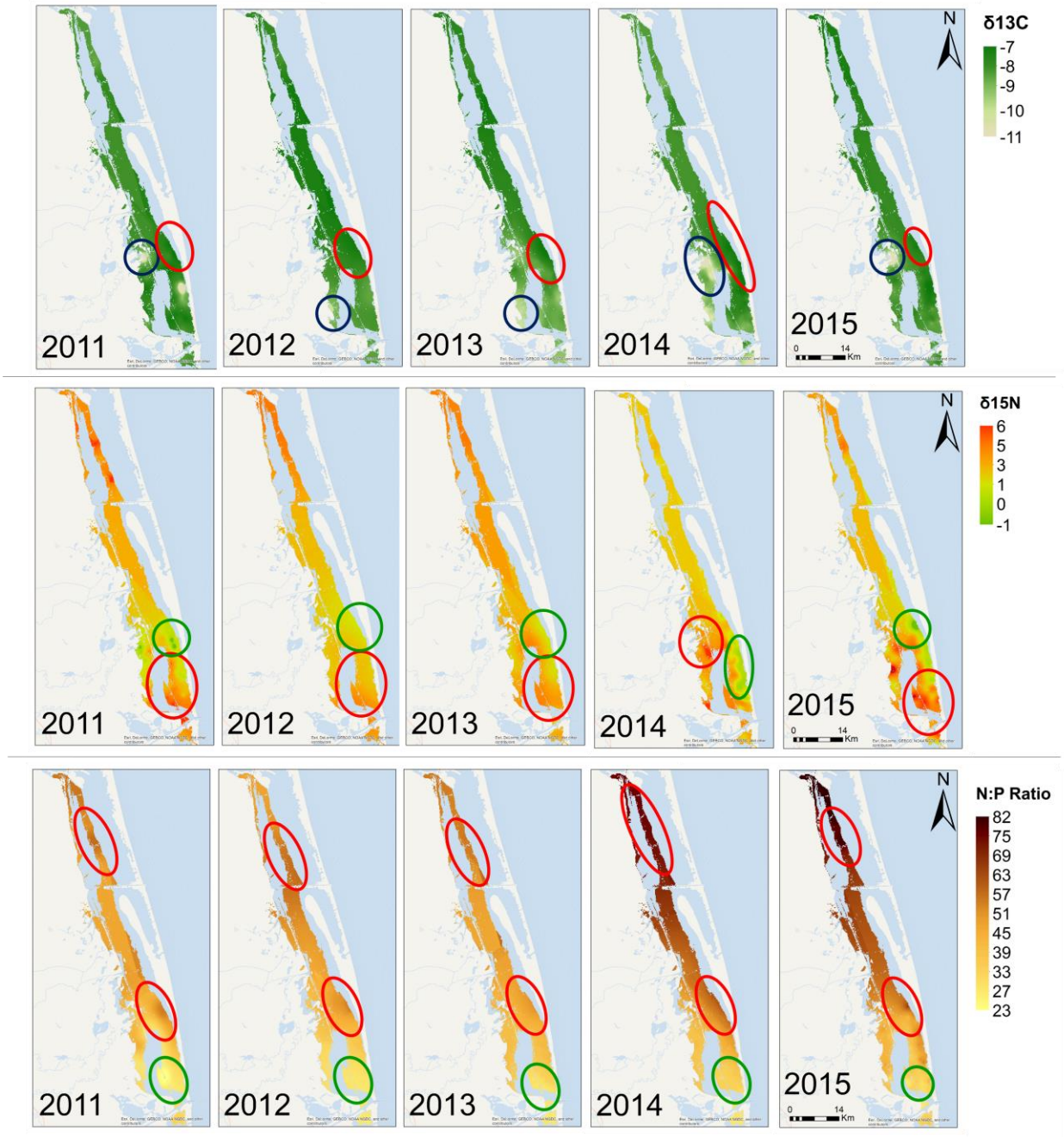

Figure 10. Pooled salinity readings collected during regular environmental monitoring 6-8 weeks prior to plant tissue collection vs. pooled *T. testudinum* $\delta^{13}C$ signatures at stations within 10 km (MACC) or 5 km (LLM), in (a) MACC and (b) LLM, 2011-2015.

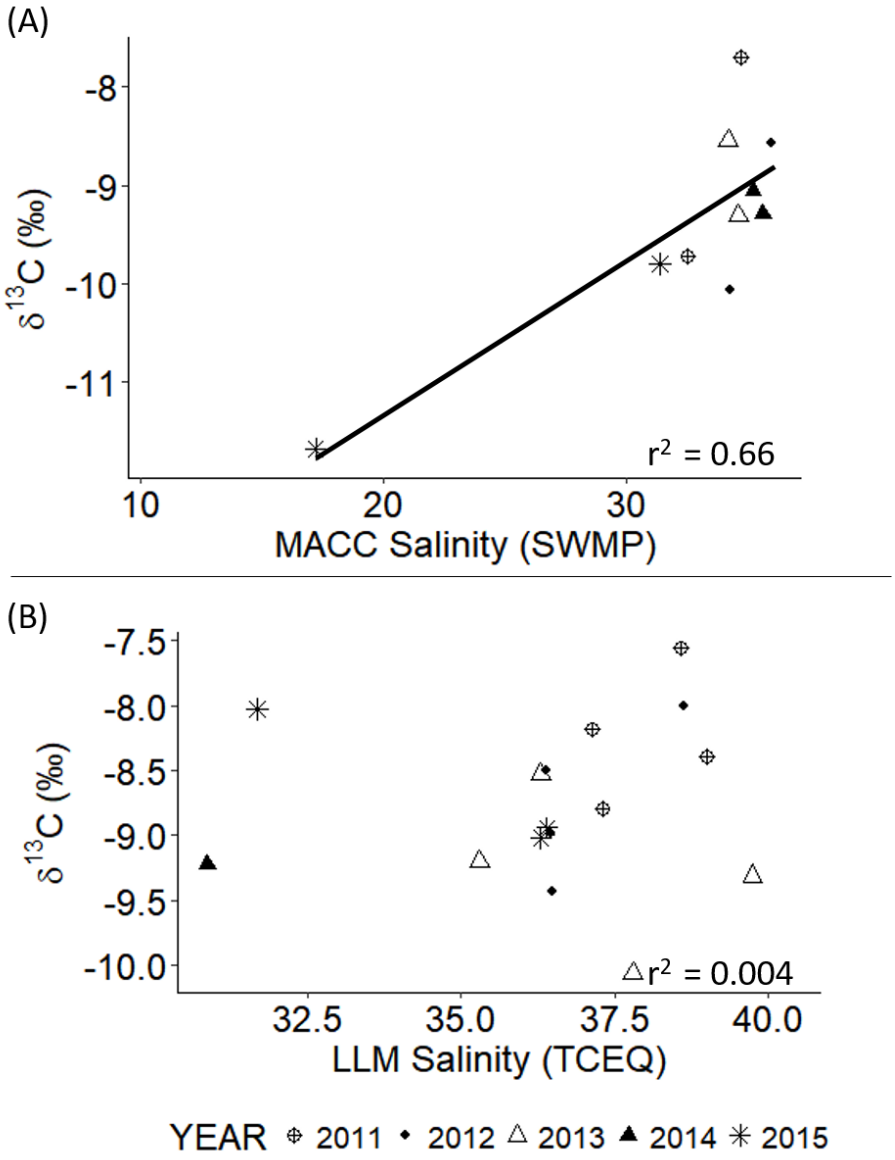

Figure 11. Pooled water column N concentrations (DIN SMWP data in the MACC, TN TCEQ data in the LLM) measured during regular environmental monitoring 6-8 weeks prior to plant tissue collection vs. pooled *T. testudinum* N:P ratios at stations within 10 km (MACC) or 5 km (LLM), in (a) MACC and (b) LLM from 2011-2015. $\delta^{15}N$ relationship with N:P ratios in (c) MACC and (d) LLM.

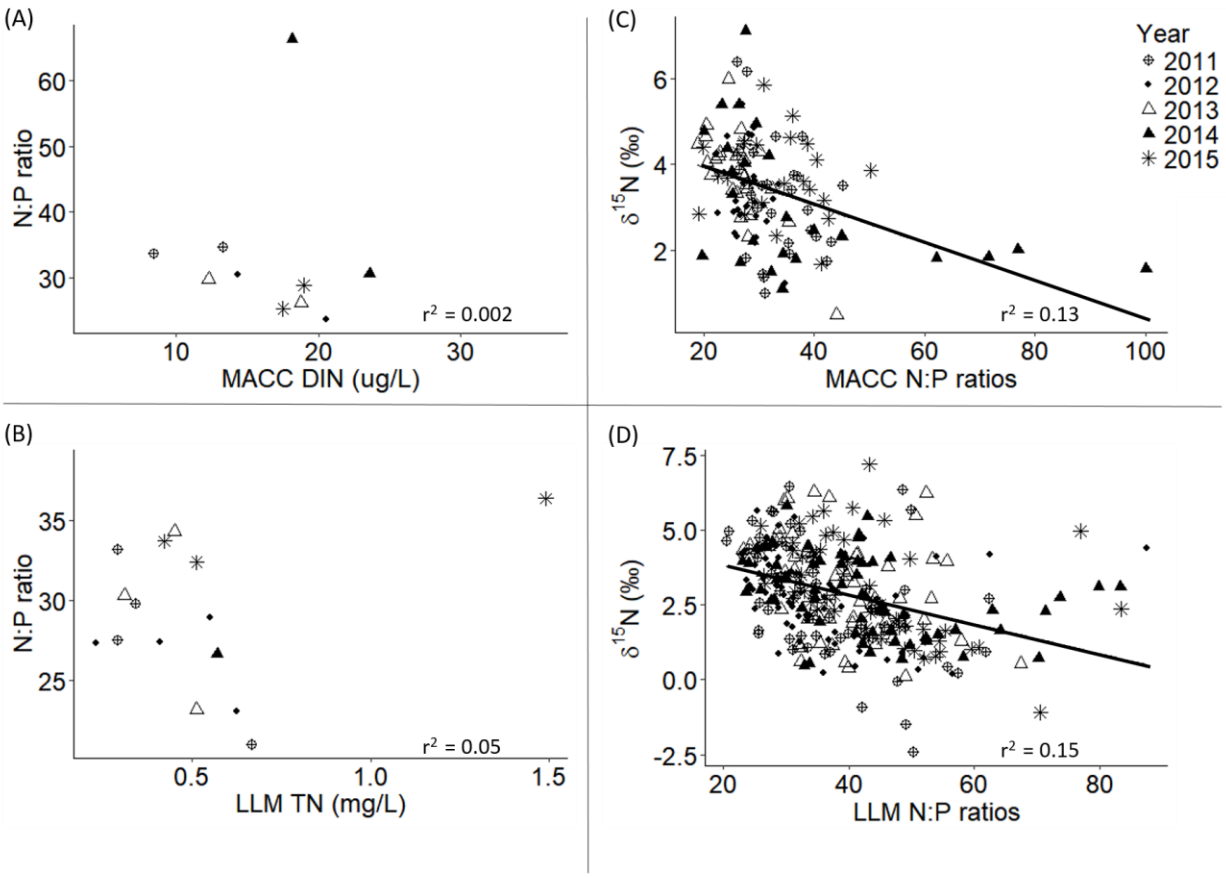

Figure 12. Land use across the lower/middle Texas coast with HUC-10 USGS watershed boundaries. Red shading is indicative of urbanized land. Stars denote significant areas of enriched $\delta^{15}N$ (red), depleted $\delta^{13}C$ (purple), and elevated N:P ratios (brown). Regressions depict the linear relationships between 1) distance from major wastewater outfall in Aransas Pass and MACC *T. testudinum* N:P ratios; 2) distance from the mouth of Baffin Bay and ULM *H. wrightii* N:P ratios; 3) distance from the mouth of an Arroyo Colorado offshoot and LLM *H. wrightii* $\delta^{15}N$; and 4) distance from the same Arroyo Colorado offshoot and LLM *H. wrightii* $\delta^{13}C$.

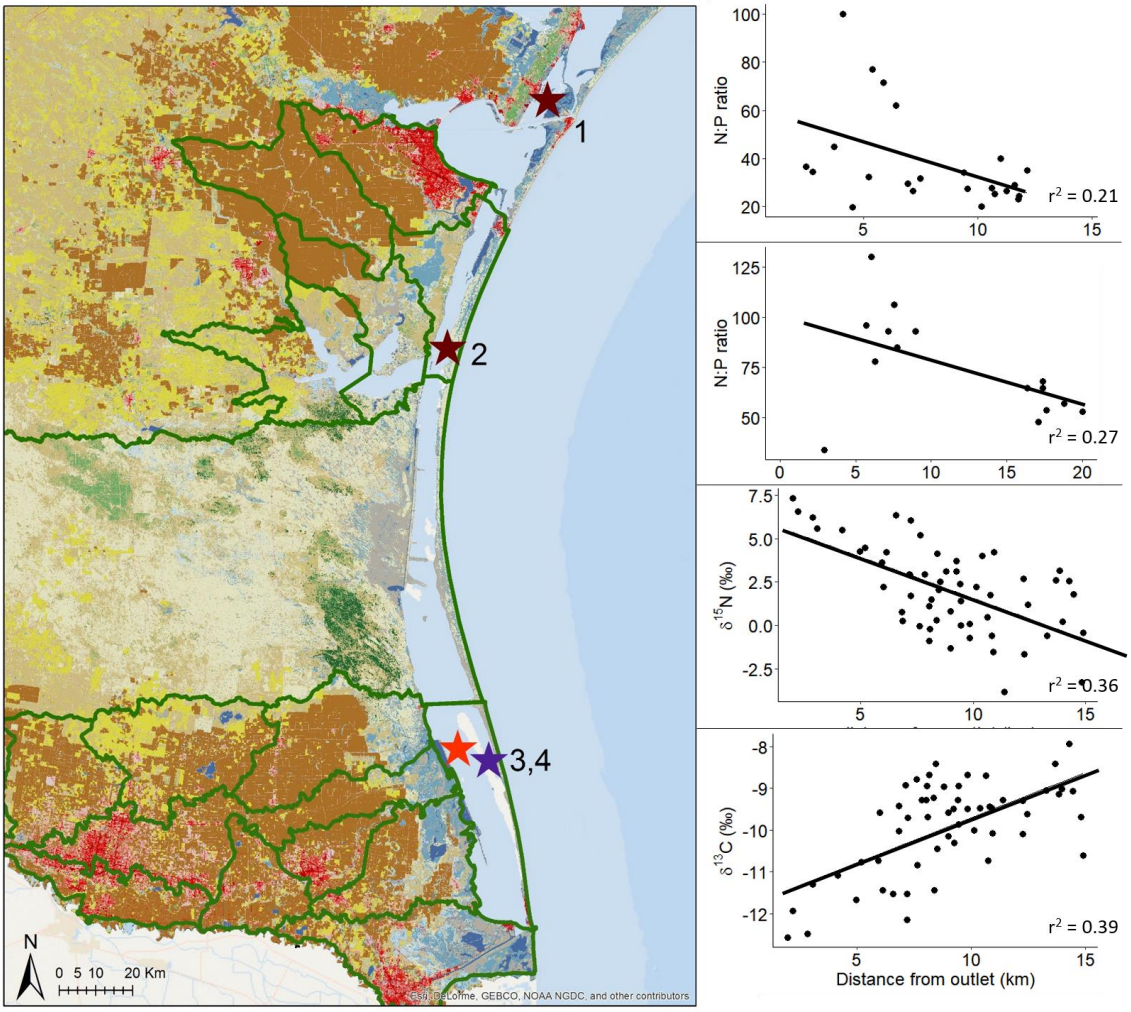

Appendix

Table 8. Cluster analysis results, *H. wrightii.* Empty cells indicate no significant clusters in that region for that year. Significance determined at $\alpha = 0.05$.

Region	Parameter	Year	High Cluster	P-value range	Std. Dev.	*n*	Low Cluster	P-value range	Std. Dev.	*n*
MACC	$\delta^{13}C$	2011	-8.66 to -8.27	0.001-0.01	0.28	2	-13.05 to -11.46	0.002-0.02	0.80	3
		2012	-9.32 to -8.14	<0.0001-0.04	0.33	13	-16.47 to -12.30	<0.0001-0.04	2.05	4
		2013	-8.91 to -8.54	0.02-0.03	0.26	2	-13.82 to -11.91	0.0001-0.0002	1.35	2
		2014	-9.41 to -7.63	<0.0001-0.02	1.00	3				
		2015	-10.81 to -9.63	<0.0001-0.005	0.46	9	-14.19 to -13.11	0.0001-0.02	0.4562	5
	$\delta^{15}N$	2011	3.62 to 7.32	<0.0001-0.04	0.96	21	-2.80 to 1.39	<0.0001-0.04	1.38	8
		2012	3.54 to 3.67	0.001-0.002	0.09	2	-5.08 to 0.43	<0.0001-0.03	1.63	12
		2013					-0.86 to 0.87	<0.0001-0.02	0.68	10
		2014					-4.06 to 0.70	<0.0001-0.04	1.86	5
		2015					-3.87 to -1.25	0.0003-0.02	1.07	5
	N:P	2011	34 to 47	<0.0001 - 0.003	4.05	9	19 to 25	0.0001-0.02	2.60	7
		2012	32 to 39	0.02-0.05	4.98	2	16 to 17	0.036-0.04	0.69	2
		2013								
		2014								
		2015	55 to 57	0.01-0.013	1.80	2	15	0.0149		1
ULM	$\delta^{13}C$	2011	-9.57 to -8.07	<0.0001-0.02	0.42	12	-14.69 to -12.78	0.0001-0.03	0.02	6
		2012	-9.17 to - 8.25	0.08-0.02	0.03	3	-12.88 to -12.0	<0.0001-0.002	0.13	3

Table 8 (continued):

ULM	$\delta^{13}C$	2013	-8.56 to -7.98	<0.0001-0.04	0.29	3				
		2014					-14.78 to -12.85	<0.00001-0.03	0.25	8
		2015	-9.62 to -8.98	0.02-0.03	0.39	2	-14.53 to -12.83	<0.0001-0.03	0.16	7
	$\delta^{15}N$	2011	3.01 to 4.18	0.0002-0.03	0.66	3	-2.52 to -0.59	0.004-0.04	0.05	5
		2012					-0.85 to 0.54	<0.0001-0.006	0.11	2
		2013	3.07 to 3.90	0.02-0.04	0.92	3	0.17	0.01		1
		2014					-3.88 to -0.77	0.0002-0.04	0.27	6
		2015	3.78 to 5.80	0.007-0.03	0.14	2	-6.20 to -1.46	0.0002-0.01	0.20	3
	N:P	2011	53 to 57	0.001-0.2	5.98	6	32	0.04		1
		2012	45 to 58	0.00002-0.03	3.00	3				
		2013	46 to 54	0.0002-0.02	2.46	3	24	0.04		1
		2014	50 to 60	0.004-0.02	2.29	3	12 to 28	<0.0001-0.04	0.09	4
		2015	78 to 130	<0.0001-0.02	15.15	7				
LLM	$\delta^{13}C$	2011	-8.72 to -6.87	<0.0001-0.04	0.49	20	-13.06 to -10.74	<0.0001-0.02	0.69	17
		2012	-8.13 to -7.15	<0.0001-0.04	0.36	9	-11.72 to -9.79	0.0001-0.04	1.07	3
		2013	-8.21 to -7.19	0.0003-0.2	0.32	11	-12.20 to -10.63	<0.0001 - 0.01	0.56	6
		2014	-8.74 to -7.33	0.0001-0.04	0.42	11	-13.96 to -11.51	<0.0001-0.003	0.89	6
		2015	-8.32 to -7.19	<0.0001 - 0.04	0.41	7	-12.77 to -10.79	0.01-0.04	0.0005	2
	$\delta^{15}N$	2011	3.62 to 7.32	<0.0001-0.04	1.13	13	-3.50 to -0.25	<0.0001-0.04	1.16	14
		2012	5.57 to 8.13	<0.0001-0.42	0.81	8	-1.60 to 0.67	0.0038-0.01	0.75	8

Table 8 (continued):

LLM	$\delta^{15}N$	2013	5.78 to 8.20	0.0004-0.04	1.13	5	-1.95 to 0.98	0.0002-0.04	1.00	7
		2014	6.54 to 10.12	<0.0001-0.04	1.77	4	-5.83 to -1.78	0.0001-0.006	2.86	2
		2015	6.56 to 9.2	0.0008-0.03	1.35	3	-4.29 to -1.20	0.009-0.04	1.42	4
	N:P	2011	56 to 74	<0.0001-0.04	5.97	8	22 to 35	0.0001-0.04	2.42	9
		2012	47 to 53	<0.0001-0.0001	3.40	3	20 to 25	0.0039-0.04	1.56	8
		2013	59 to 66	<0.0001-0.0002	4.61	2	22 to 23	0.0005-0.005	0.57	3
		2014	69 to 73	0.02-0.03	2.70	2	30.2156	0.03		1
		2015	68 to 104	<0.0001-0.03	13.47	6	22 to 44	<0.0001-0.04	7.30	9

Table 9. Tukey post-hoc pairwise interannual comparisons for $\delta^{13}C$, $\delta^{15}N$, and N:P ratios, *H. wrightii*. Significant relationships ($p < 0.05$) are denoted by an asterisk (*).

$\delta^{13}C$ Tukey Post-Hoc Tests – MACC *H. wrightii T.*				
	Estimate	*Std. Error*	*z-value*	*p-value*
2015-2011	-1.48	0.2	-7.58	<0.0001*
2015-2012	-1.3	0.21	-6.31	<0.0001*
2015-2013	-1.57	0.22	-7.32	<0.0001*
2015-2014	-1.39	0.22	-6.41	<0.0001*
2013-2012	0.27	0.2	1.36	0.65
2012-2011	-0.18	0.17	-1.05	0.83
2014-2013	-0.19	0.21	-0.89	0.9
2014-2011	-0.1	0.19	-0.52	0.99
2012-2011	0.09	0.19	0.47	0.99
2014-2012	0.08	0.2	0.41	0.99
$\delta^{15}N$ Tukey Post-Hoc Tests – MACC *H. wrightii*				
	Estimate	*Std. Error*	*z-value*	*p-value*
2015-2013	-1.13	0.28	-3.98	<0.001*
2015-2014	-0.98	0.29	-3.43	0.01*
2013-2011	0.78	0.25	3.1	0.02*
2014-2011	0.63	0.26	2.43	0.11
2013-2012	0.56	0.26	2.12	0.21
2015-2012	-0.57	0.27	-2.1	0.22
2014-2012	0.4	0.27	1.5	0.56
2015-2011	-0.35	0.26	-1.34	0.67
2012-2011	0.22	0.23	0.96	0.87
2014-2013	-0.16	0.28	-0.56	0.98
N:P ratio Tukey Post-Hoc Tests – MACC *H. wrightii*				
	Estimate	*Std. Error*	*z-value*	*p-value*
2012-2011	-4.76	1.14	-4.19	<0.001*
2015-2012	9.55	1.36	7.03	<0.001*
2015-2013	8.89	1.42	6.28	<0.001*
2015-2011	4.79	1.26	3.79	0.001*
2012-2012	4.89	1.34	3.65	0.002*
2013-2011	-4.1	1.22	-3.37	0.007*

Table 9 (continued):

2015-2014	4.66	1.43	3.26	0.01*
2014-2013	4.23	1.4	3.02	0.02*
2013-2012	0.66	1.32	0.51	0.99
2014-2011	0.13	1.25	0.1	1
δ^{13}C Tukey Post-Hoc Tests – ULM *H. wrightii*				
	Estimate	*Std. Error*	*z-value*	*p-value*
2012-2011	0.84	0.17	4.91	<0.0001*
2013-2012	-0.82	0.18	-4.42	<0.0001*
2014-2012	-1.52	0.19	-8.06	<0.0001*
2015-2012	-1	0.2	-5.13	<0.0001*
2014-2011	-0.69	0.18	-3.88	0.001*
2014-2013	-0.71	0.19	-3.71	0.002*
2015-2014	0.52	0.2	2.61	0.07
2015-2013	-0.19	0.2	-0.95	0.87
2015-2011	-0.17	0.18	-0.91	0.89
2013-2011	0.02	0.17	0.12	1
δ^{15}N Tukey Post-Hoc Tests – ULM *H. wrightii*				
	Estimate	*Std. Error*	*z-value*	*p-value*
2012-2011	1.39	0.21	6.54	<0.001*
2014-2012	-1.17	0.24	-4.82	<0.001*
2015-2012	-1.03	0.25	-4.14	<0.001*
2013-2011	0.8	0.21	3.74	0.002*
2013-2012	-0.59	0.24	-2.48	0.09
2014-2013	-0.58	0.24	-2.38	0.12
2015-2013	-0.45	0.25	-1.78	0.38
2015-2011	0.36	0.23	1.55	0.53
2014-2011	0.22	0.22	1.01	0.85
2015-2014	0.13	0.25	0.52	0.99
N:P ratio Tukey Post-Hoc Tests – ULM *H. wrightii*				
	Estimate	*Std. Error*	*z-value*	*p-value*
2012-2011	-10.09	1.63	-6.2	<0.001*
2013-2011	-10.6	1.63	-6.51	<0.001*
2015-2012	30.03	1.9	15.82	<0.001*

Table 9 (continued):

2015-2013	30.54	1.9	16.07	<0.001*
2015-2014	24.81	1.94	12.77	<0.001*
2015-2011	19.93	1.73	11.52	<0.001*
2014-2013	5.72	1.87	3.06	0.02*
2014-2011	-4.88	1.7	-2.87	0.03*
2014-2012	5.22	1.87	2.79	0.04
2013-2012	-0.51	1.81	-0.28	1
δ^{13}C Tukey Post-Hoc Tests – LLM *H. wrightii*				
	Estimate	*Std. Error*	*z-value*	*p-value*
2012-2011	0.79	0.11	7.44	<0.001*
2014-2012	-0.95	0.11	-8.35	<0.001*
2015-2012	-0.8	0.12	-6.84	<0.001*
2014-2013	-0.52	0.12	-4.51	<0.001*
2013-2012	-0.43	0.11	-3.75	0.002*
2013-2011	0.36	0.11	3.27	0.01*
2015-2013	-0.38	0.12	-3.15	0.01*
2014-2011	-0.16	0.11	-1.47	0.58
2015-2014	0.14	0.12	1.22	0.74
2015-2011	-0.02	0.11	-1.47	1
δ^{15}N Tukey Post-Hoc Tests – LLM *H. wrightii*				
	Estimate	*Std. Error*	*z-value*	*p-value*
2012-2011	1.47	0.18	8.38	<0.001*
2013-2011	1.5	0.18	8.19	<0.001*
2014-2011	1.75	0.18	9.59	<0.001*
2015-2011	0.94	0.19	4.99	<0.001*
2015-2014	-0.81	0.2	-4.11	<0.001*
2015-2013	-0.55	0.2	-2.82	0.04*
2015-2012	-0.53	0.19	-2.74	0.05
2014-2012	0.28	0.19	1.49	0.57
2014-2013	0.26	0.19	1.33	0.67
2013-2012	0.03	0.19	0.14	1

Table 9 (continued):

N:P ratio Tukey Post-Hoc Tests – LLM *H. wrightii*				
	Estimate	*Std. Error*	*z-value*	*p-value*
2012-2011	-13.37	1.38	-9.68	<0.001*
2015-2011	9.04	1.46	6.18	<0.001*
2013-2012	9.66	1.52	6.36	<0.001*
2014-2012	16.46	1.52	10.8	<0.001*
2015-2012	22.41	1.55	14.44	<0.001*
2014-2013	6.8	1.54	4.41	<0.001*
2015-2013	12.76	1.57	8.11	<0.001*
2015-2014	5.96	1.58	3.78	0.001*
2013-2011	-3.72	1.43	-2.61	0.07
2014-2011	3.08	1.42	2.17	0.19

Table 10. Cluster analysis results, *T. testudinum*. Empty cells denote no significant clusters in that region for that year. Significance determined at $\alpha = 0.05$.

Region	Parameter	Year	High Cluster	P-value range	Std. Dev.	*n*	Low Cluster	P- value range	Std. Dev.	*n*
MACC	$\delta^{13}C$	2011								
		2012					-11.28 to -10.94	0.004-0.008	0.24	2
		2013								
		2014								
		2015								
	$\delta^{15}N$	2011								
		2012								
		2013								
		2014	3.84 to 7.12	<0.0001-0.04	1.12	7	1.49 to 1.86	0.3-0.04	0.18	4
		2015					1.68 to 2.33	0.002-0.01	0.46	2
	N:P	2011								
		2012	31 to 34	0.0234-0.04	1.55	2				
		2013								
		2014	62 to 100	<0.0001-0.002	16.14	4				
		2015					19 to 20	0.004-0.03	0.56	2
LLM	$\delta^{13}C$	2011	-7.42 to -6.70	0.0004-0.03	0.30	4	-11.31 to -10.0	<0.0001-0.03	0.52	7
		2012	-7.47 to -6.31	<0.0001-0.0003	0.39	7	-10.64 to -9.21	<0.0001-0.01	0.51	5
		2013	-7.39 to -6.23	<0.001-0.01	0.47	7	-10.61 to -9.17	<0.0001-0.02	0.54	8
		2014	-8.32 to -6.94	<0.0001-0.04	0.40	14	-11.76 to -9.87	<0.0001-0.02	0.65	8
		2015	-7.59 to -6.35	<0.0001-0.04	0.44	6	-11.77 to -11.06	<0.0001	0.50	2
	$\delta^{15}N$	2011	3.62 to 7.32	<0.0001-0.04	0.96	21	-2.39 to 1.39	<0.0001-0.04	1.38	8
		2012	4.19 to 5.65	<0.0001-0.03	0.56	6	0.21 to 1.18	<0.0001-0.02	0.32	8
		2013	4.35 to 5.99	<0.0001-0.04	0.69	7	0.39 to 1.64	0.002-0.04	0.50	6
		2014	3.88 to 5.81	<0.0001-.04	0.83	6	0.68 to 1.56	<0.0001-0.01	0.32	10

Table 10 (continued):

LLM	$\delta^{15}N$	2015	4.81 to 6.37	<0.0001-0.01	0.57	6	-1.08 to 1.68	<0.0001-0.02	0.74	10
	N:P	2011	43 to 62	<0.0001-0.04	6.04	13	20 to 29	<0.0001-0.01	2.49	14
		2012	42 to 87	<0.0001-0.04	13.21	9	23 to 29	<0.0001-0.03	1.72	11
		2013	47 to 67	<0.0001-0.04	6.13	8	23 to 32	<0.0001-0.03	3.20	10
		2014	52 to 83	<0.0001-0.04	10.35	11	23 to 34	<0.0001-0.04	3.06	9
		2015	54 to 83	<0.0001-0.03	12.4	4	26 to 34	0.01-0.03	3.05	5

Table 11. Tukey post-hoc pairwise interannual comparisons for $\delta^{13}C$, $\delta^{15}N$, and N:P ratios, *T. testudinum*. Significant relationships ($p < 0.05$) are denoted by an asterisk (*).

$\delta^{13}C$ Tukey Post-Hoc Tests – MACC *T. testudinum*				
	Estimate	*Std. Error*	*z-value*	*p-value*
2015-2011	-1.51	0.24	-6.41	<0.0001*
2015-2012	-1.11	0.23	-4.74	<0.0001*
2015-2013	1.36	0.24	-5.78	<0.0001*
2015-2014	-1.13	0.24	-4.7	<0.0001*
2012-2011	-0.4	0.23	-1.79	0.38
2014-2011	-0.38	0.23	-1.64	0.47
2013-2012	0.25	0.23	1.13	0.79
2014-2013	-0.24	0.23	-1.01	0.85
2013-2011	-0.15	0.23	-0.65	0.97
2014-2012	0.02	0.23	0.08	1
$\delta^{15}N$ Tukey Post-Hoc Tests – MACC *T. testudinum*				
	Estimate	*Std. Error*	*z-value*	*p-value*
2014-2013	-0.77	0.26	-2.96	0.03*
2015-2014	0.71	0.26	2.68	0.06
2013-2011	0.61	0.25	2.44	0.1
2015-2011	0.56	0.26	2.13	0.21
2013-2012	0.44	0.25	1.76	0.4
2015-2012	0.38	0.26	1.47	0.58
2014-2012	-0.33	0.26	-1.28	0.7
2012-2011	0.17	0.25	0.7	0.96
2014-2011	-0.15	0.26	-0.6	0.98
2015-2013	-0.06	0.26	-0.22	1
N:P ratio Tukey Post-Hoc Tests – MACC *T. testudinum*				
	Estimate	*Std. Error*	*z-value*	*p-value*
2014-2013	11.27	2.84	3.97	<0.001*
2014-2012	9.87	2.79	3.54	0.004*
2013-2011	-7.33	2.76	-2.66	0.06
2015-2013	6.31	2.84	2.22	0.17
2012-2011	-5.93	2.71	-2.19	0.18
2015-2012	4.9	2.79	1.76	0.4
2015-2014	-4.97	2.9	-1.71	0.42
2014-2011	3.94	2.82	1.4	0.63
2013-2012	-1.4	2.73	-0.51	0.99

Table 11 (continued):

2015-2011	-1.03	2.82	-0.37	1
δ^{13}C Tukey Post-Hoc Tests - LLM *T. testudinum*				
	Estimate	*Std. Error*	*z-value*	*p-value*
2014-2012	-0.55	0.15	-3.7	0.002*
2014-2011	-0.48	0.15	-3.27	0.01*
2014-2013	-0.43	0.15	-2.91	0.03*
2015-2012	-0.17	0.15	-1.1	0.81
2015-2014	0.38	0.15	2.5	0.9
2013-2012	-0.12	0.15	-0.82	0.93
2015-2011	-0.1	0.15	-0.67	0.96
2012-2011	0.07	0.15	0.45	0.99
2013-2011	-0.05	0.15	-0.37	1
2015-2013	-0.05	0.15	-0.31	1
δ^{15}N Tukey Post-Hoc Tests – LLM *T. testudinum*				
	Estimate	*Std. Error*	*z-value*	*p-value*
2013-2012	0.35	0.19	1.88	0.33
2015-2012	0.36	0.19	1.86	0.34
2013-2011	0.34	0.18	1.84	0.35
2015-2011	0.35	0.19	1.83	0.36
2014-2013	-0.29	0.19	-1.53	0.55
2015-2014	0.3	0.19	1.53	0.55
2014-2012	0.07	0.19	0.35	1
2014-2011	0.05	0.19	0.29	1
2015-2013	0.01	0.19	0.06	1
2012-2011	-0.01	1.87	-0.06	1
N:P ratio Tukey Post-Hoc Tests - LLM *T. testudinum*				
	Estimate	*Std. Error*	*z-value*	*p-value*
2014-2011	6.25	1.25	5.01	<0.001*
2015-2011	6.5	1.29	5.03	<0.001*
2014-2012	7.02	1.27	5.54	<0.001*
2015-2012	7.26	1.31	5.55	<0.001*
2015-2013	4.05	1.3	3.12	0.02*
2014-2013	3.8	1.25	3.04	0.02*
2013-2012	3.21	1.25	2.56	0.08
2013-2011	2.45	1.24	1.98	0.28

Table 11 (continued):

2012-2011	-0.76	1.25	-0.61	0.97
2015-2014	0.24	1.3	0.19	1

Figure 13. C:N biplot, *H. wrightii* (black) and *T. testudinum* (blue) in all regions

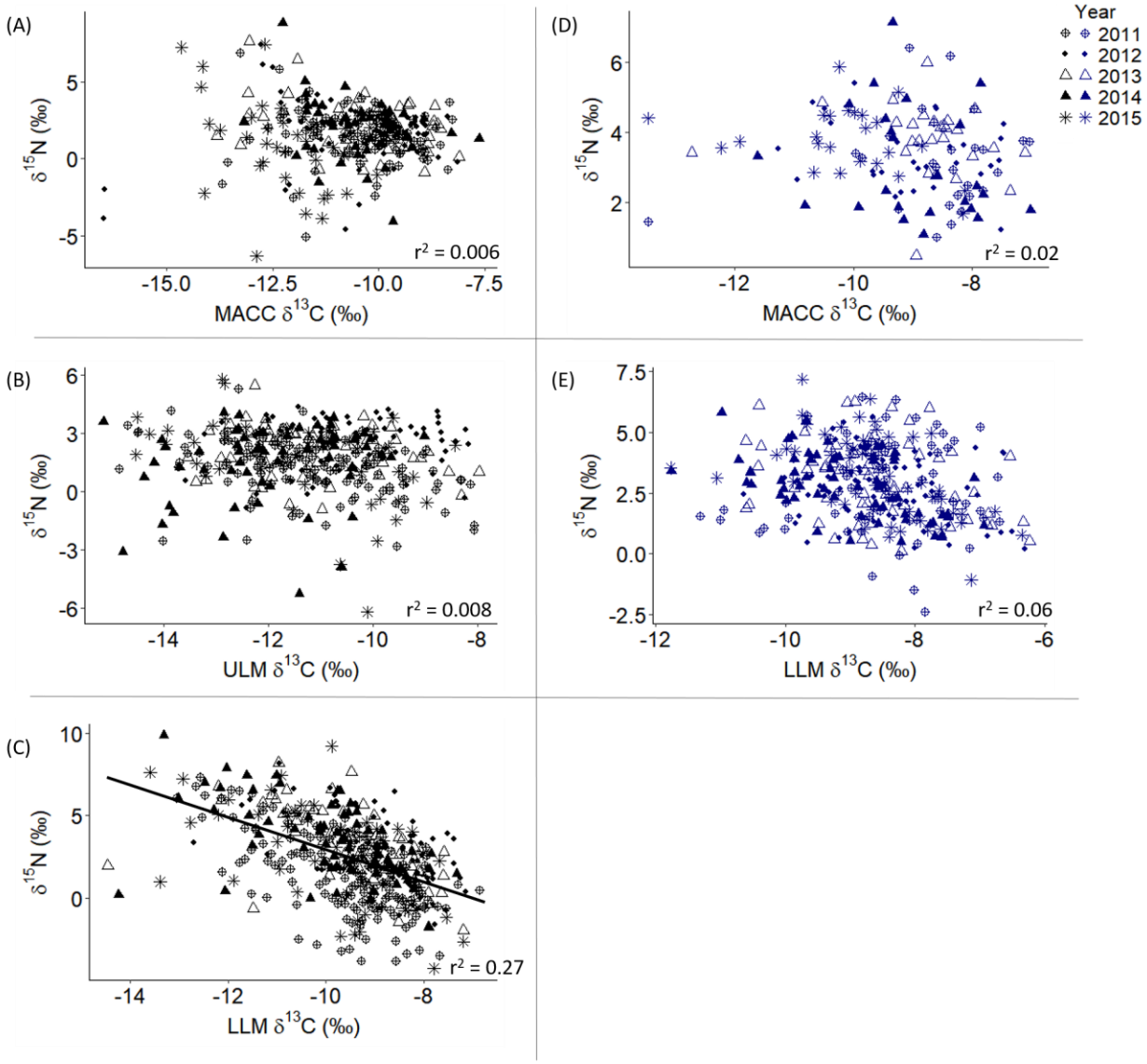

Figure 14. Environmental data collected during Tier-2 sampling vs. *H. wrightii* $\delta^{13}C$ signatures: MACC, ULM, and LLM, 2011-2015.

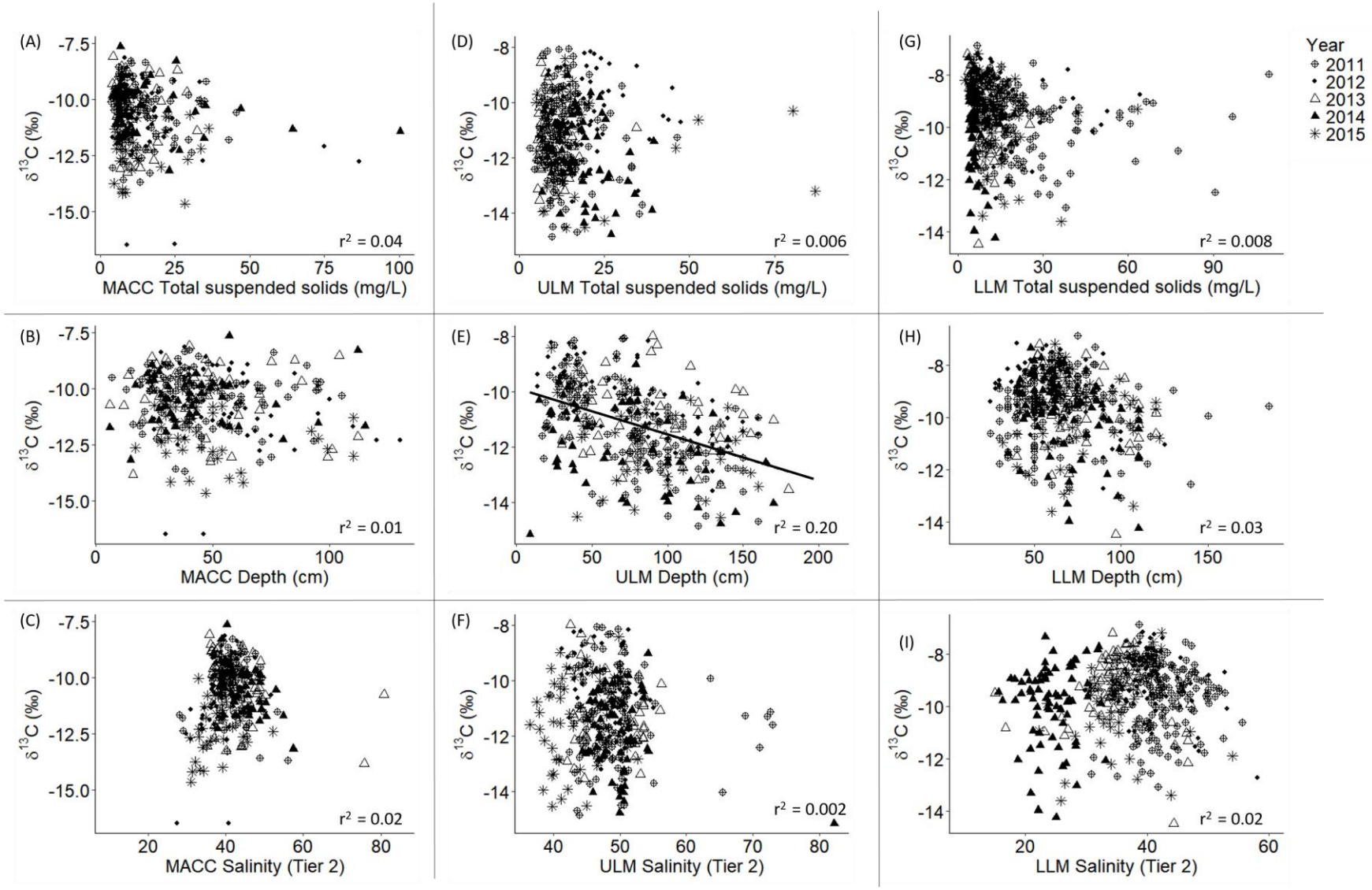

Figure 15. Pooled chlorophyll-*a* concentrations measured during regular environmental monitoring 6-8 weeks prior to plant tissue collection vs. pooled *H. wrightii* $\delta^{13}C$ signatures at stations within 10 km (MACC) or 5 km (ULM/LLM), in (a) MACC, (b) ULM, and (c) LLM from 2011-2015.

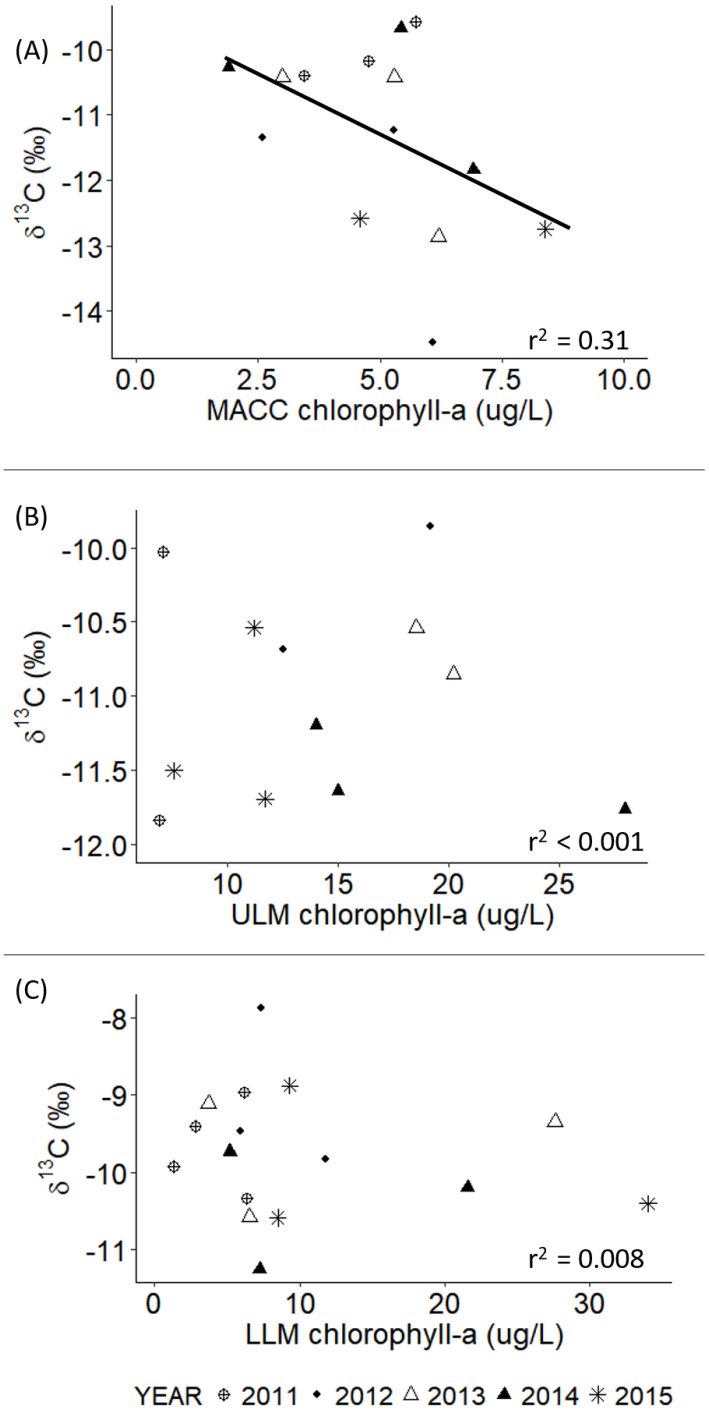

Figure 16. Environmental data collected during Tier-2 sampling vs. *T. testudinum* $\delta^{13}C$ signatures: MACC and LLM, 2011-2015. No relationships are significant.

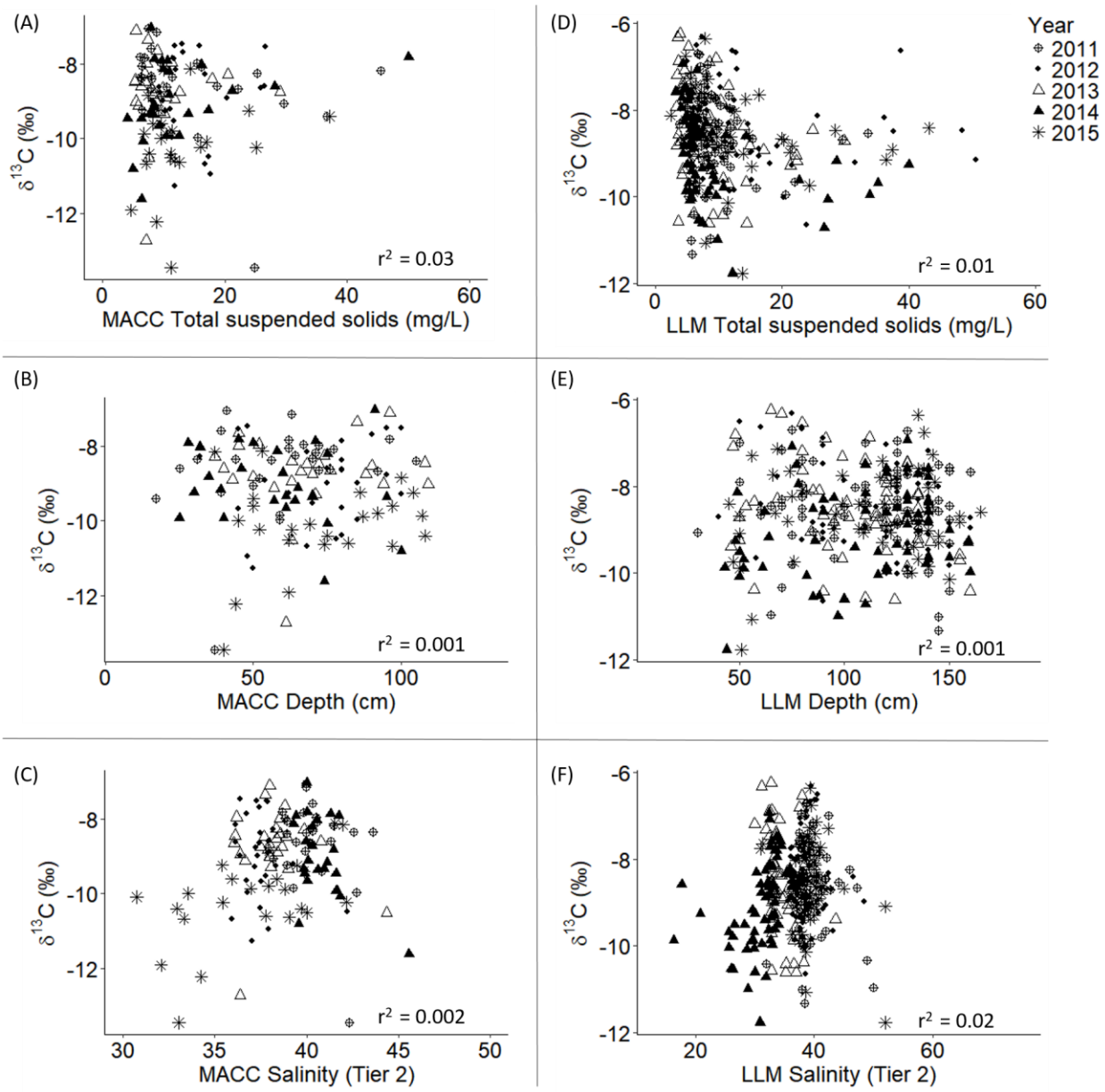

Figure 17. Pooled chlorophyll-*a* concentrations measured during regular environmental monitoring 6-8 weeks prior to plant tissue collection vs. pooled *T. testudinum* $\delta^{13}C$ signatures at stations within 10 km (MACC) or 5 km (ULM/LLM), in (a) MACC and (b) LLM from 2011-2015.

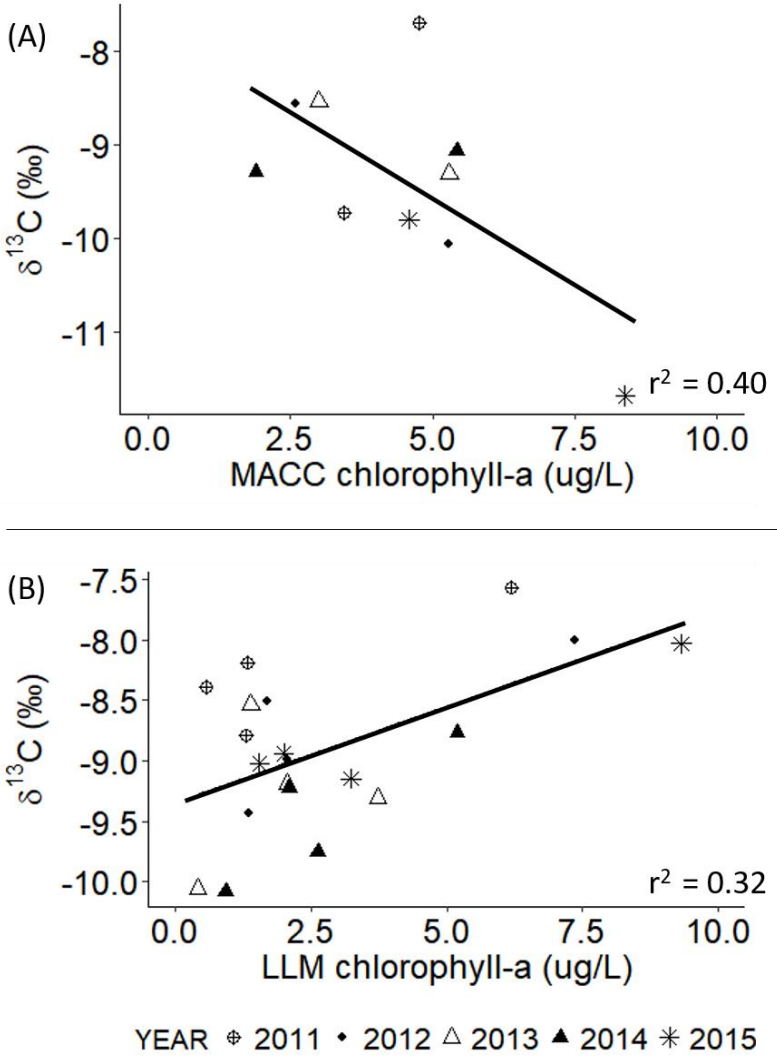

References

Ackerman, J.D., & Okubo, A. (1993). Reduced mixing in a marine macrophyte canopy. *Functional Ecology, 7*(3), 305–309. https://doi.org/10.2307/2390209.

An, S., & Gardner, W.S. (2002). Dissimilatory nitrate reduction to ammonium (DNRA) as a nitrogen link, versus denitrification as a sink in a shallow estuary (Laguna Madre/Baffin Bay, Texas). *Marine Ecology Progress Series, 237*, 41–50.

Anderson, W.T., & Fourqurean, J.W. (2003). Intra- and interannual variability in seagrass carbon and nitrogen stable isotopes from south Florida, a preliminary study. *Organic Geochemistry*, *34*(2), 185–194. https://doi.org/10.1016/S0146-6380(02)00161-4.

Armitage, A.R., Frankovich, T.A., Heck, K.L., & Fourqurean, J.W. (2005). Experimental nutrient enrichment causes complex changes in seagrass, microalgae, and macroalgae community structure in Florida Bay. *Estuaries, 28*(3), 422–434. https://doi.org/10.1007/BF02693924.

Atkinson, M.J., & Smith. S.V. (1984). C:N:P ratios of benthic marine plants. *Limnology and Oceanography, 28*, 568-574.

Beck, M.W., Heck, K.L., Able, K.W., Childers, D.L., Eggleston, D.B., Gillanders, B.M., … Weinstein, M.P. (2001). The identification, conservation, and management of estuarine and marine nurseries for fish and fnvertebrates: A better understanding of the habitats that serve as nurseries for marine species and the factors that create site-specific variability in nursery quality will improve conservation and management of these areas. *BioScience, 51*(8), 633–641.

Bishop, K.A., McClelland, J.W., & Dunton, K.H. (2017). Freshwater contributions and nitrogen sources in a south Texas estuarine ecosystem: a time-integrated perspective from stable isotopic ratios in the eastern oyster (*Crassostrea virginica*). *Estuaries and Coasts, 40*(5), 1314–1324. https://doi.org/10.1007/s12237-017-0227-0.

Bowen, G.J. (2010). Isoscapes: spatial pattern in isotopic biogeochemistry. *Annual Review of Earth and Planetary Sciences*, *38*(1), 161–187. https://doi.org/10.1146/annurev-earth-040809-152429.

Brock, D.A. (2001). Nitrogen budget for low and high freshwater inflows, Nueces Estuary, Texas. *Estuaries, 24*(4), 509–521. https://doi.org/10.2307/1353253.

Brown, J.L.F., J.L. Brewton, T.J. Evans, J.H. McGowen, W.A. White, C.G. Groat, and W.L. Fisher. (1980). Environmental Geologic Atlas of the Texas Coastal Zone-

Brownsville-Harlingen Area. Austin, TX: Bureau of Economic Geology—The University of Texas at Austin.

Brush, M.J. & S.W. Nixon. (2002). Direct measurements of light attenuation by epiphytes on eelgrass *Zostera marina*. *Marine Ecology Progress Series, 238*, 73–79.

Burkholder D.A., Fourqurean J.W., & Heithaus M.R. (2013). Spatial pattern in seagrass stoichiometry indicates both N-limited and P-limited regions of an iconic P-limited subtropical bay. *Marine Ecology Progress Series 472*, 101–115.

Campbell, J.E., & Fourqurean, J.W. (2009). Interspecific variation in the elemental and stable isotope content of seagrasses in South Florida. *Marine Ecology Progress Series 387*, 109-123.

Campbell J.E., & Fourqurean J.W. (2013). Mechanisms of bicarbonate use influence the photosynthetic carbon dioxide sensitivity of tropical seagrasses. *Limnology and Oceanography, 58(*3), 839–848. https://doi.org/10.4319/lo.2013.58.3.0839.

Carriquiry, J. D., Jorgensen, P., Villaescusa, J. A., & Ibarra-Obando, S. E. (2016). Isotopic and elemental composition of marine macrophytes as biotracers of nutrient recycling within a coastal lagoon in Baja California, Mexico. *Estuaries and Coasts, 39*(2), 451–461. https://doi.org/10.1007/s12237-015-9992-9.

Ceburnis, D., Masalaite, A., Ovadnevaite, J., Garbaras, A., Remeikis, V., Maenhaut, W., … O'Dowd, C.D. (2016). Stable isotopes measurements reveal dual carbon pools contributing to organic matter enrichment in marine aerosol. *Scientific Reports, 6*, 36675.

Chapman, H.D., & Pratt, P.F. (1961). Methods of Analysis for Soils, Plants and Water. Berkley, CA: Univ. California, Berkeley.

Christiaen, B., Bernard, R. J., Mortazavi, B., Cebrian, J., & Ortmann, A. C. (2014). The degree of urbanization across the globe is not reflected in the $\delta^{15}N$ of seagrass leaves. *Seagrass Meadows in a Globally Changing Environment, 83*(2), 440–445. https://doi.org/10.1016/j.marpolbul.2013.06.024.

Cook, C.D.L. (1998). Hydrocharitaceae. In *The Families and Genera of Vascular Plants book series (FAMILIES GENERA, volume 4): Flowering Plants · Monocotyledons, Alismatanae and Commelinanae (except Gramineae).* Edited by K. Kubitzki. Berlin: Springer. 234 – 248 pp. https://doi.org/10.1007/978-3-662-03531-3.

Cooper, L.W., & DeNiro, M.J. (1989). Stable carbon isotope variability in the seagrass *Posidonia oceanica*: evidence for light intensity effects. *Marine Ecology Progress Series, 50*(3), 225–229.

Costanzo, S. D., O'Donohue, M. J., Dennison, W. C., Loneragan, N. R., & Thomas, M. (2001). A new approach for detecting and mapping sewage impacts. *Marine Pollution Bulletin*, *42*(2), 149–156. https://doi.org/10.1016/S0025-326X(00)00125-9.

Dawes, C.J. 1998. *Marine Botany.* 2nd edition. New York: John C. Wiley & Sons.

Dawson, T.E., Mambelli, S., Plamboeck, A.H., Templer, P.H., & Tu, K.P. (2002). Stable isotopes in plant ecology. *Annual Review of Ecology and Systematics*, *33*(1), 507–559. https://doi.org/10.1146/annurev.ecolsys.33.020602.095451.

del Castillo, J., Aguilera, M., Voltas, J, & Ferrio, J.P. (2013). Isoscapes of tree-ring carbon-13 perform like meteorological networks in predicting regional precipitation patterns. *Journal of Geophysical Research: Biogeosciences, 118*(1), 352–360. https://doi.org/10.1002/jgrg.20036.

Denk, T.R.A., Mohn, J., Decock, C., Lewicka-Szczebak, D., Harris, E., Butterbach-Bahl, K., … Wolf, B. (2017). The nitrogen cycle: a review of isotope effects and isotope modeling approaches. *Soil Biology and Biochemistry*, *105*, 121–137. https://doi.org/10.1016/j.soilbio.2016.11.015.

DeYoe, H., Pulich, W., & Fernando, N. (2016). Modeled inflow validation & nutrient loading estimation in two subwatersheds of the Lower Laguna Madre. Austin, TX: Texas General Land Office.

Diener, R. A. (1975). Cooperative Gulf of Mexico estuarine inventory and study - Texas: area description. NOAA Technical Report NMFS CIRC-393. U.S. Dept. of Commerce, National Oceanic and Atmospheric Administration. Seattle, WA.

Duarte, C. M. (1990). Seagrass nutrient content. *Marine Ecology Progress Series*, *67*(2), 201–207.

Duarte, C.M. (2002). The future of seagrass meadows. *Environmental Conservation 29*(2), 192-206.

Dunton, K. H. (1990). Production ecology of *Ruppia maritima* L. s.l. and *Halodule wrightii* Aschers, in two subtropical estuaries. *Journal of Experimental Marine Biology and Ecology*, *143*(3), 147–164. https://doi.org/10.1016/0022-0981(90)90067-M.

Dunton, K.H. (1994). Seasonal growth and biomass of the subtropical seagrass *Halodule wrightii* in relation to continuous measurements of underwater irradiance. *Marine Biology 120*(3), 479–489. doi:10.1007/BF00680223.

Dunton, K.H. (1996). Photosynthetic production and biomass of the subtropical seagrass *Halodule wrightii* along an estuarine gradient. *Estuaries 19*(2), 436–447. doi:10.2307/1352461.

Dunton, K.H., Pulich, W. Mutchler, T. (2011). A seagrass monitoring program for Texas coastal waters: multiscale integration of landscape features with plant and water quality indicators. Corpus Christi, TX: Coastal Bend Bays & Estuaries Program.

Durako, M. J. (1993). Photosynthetic utilization of $CO_{2(aq)}$ and HCO_3^- in *Thalassia testudinum* (Hydrocharitaceae). *Marine Biology*, *115*(3), 373–380. https://doi.org/10.1007/BF00349834.

Ferdie, M., & Fourqurean J.W. (2004). Responses of seagrass communities to fertilization along a gradient of relative availability of nitrogen and phosphorus in a carbonate environment. *Limnology and Oceanography*, *49*(6), 2082–2094. https://doi.org/10.4319/lo.2004.49.6.2082.

Fonseca, M.S., Fisher, J.S., Zieman, J.C., Thayer, G.W. (1982). Influence of the seagrass *Zostera marina* (L.) on current flow. *Estuarine, Coastal and Shelf Science 15*, 351-364.

Fourqurean, J. W., Duarte, C. M., Kennedy, H., Marba, N., Holmer, M., Mateo, M. A., … Serrano, O. (2012). Seagrass ecosystems as a globally significant carbon stock. *Nature Geosci*, *5*(7), 505–509. https://doi.org/10.1038/ngeo1477.

Fourqurean, J.W., Escorcia, S.P., Anderson, W.T., & Zieman, J.C. (2005). Spatial and seasonal variability in elemental content, $\delta^{13}C$, and $\delta^{15}N$ of *Thalassia testudinum* from South Florida and its implications for ecosystem studies. *Estuaries, 28*(3), 447–461. https://doi.org/10.1007/BF02693926.

Fourqurean, J. W., George V. N. Powell, Kenworthy, W. J., & Zieman, J. C. (1995). The effects of long-term manipulation of nutrient supply on competition between the seagrasses *Thalassia testudinum* and *Halodule wrightii* in Florida Bay. *Oikos, 72*(3), 349–358. https://doi.org/10.2307/3546120.

Fourqurean, J.W., Manuel, S.A., Coates, K.A., Kenworthy, W.J., & Boyer, J.N. (2015). Water quality, isoscapes and stoichioscapes of seagrasses indicate general P

limitation and unique N cycling in shallow water benthos of Bermuda. *Biogeosciences, 12*(20), 6235–6249. https://doi.org/10.5194/bg-12-6235-2015.

Fourqurean J.W., Moore, T.O., Fry, B., & Hollibaugh, J.T. (1997). Spatial and temporal variation in C:N:P ratios, $\delta^{15}N$ and $\delta^{13}C$ of eelgrass *Zostera marina* as indicators of ecosystem processes, Tomales Bay, California, USA. *Marine Ecology Progress Series 157*, 147–157.

Fourqurean J. W., Zieman, J.C., & Powell, G.V.N. (1992). Phosphorus limitation of primary production in Florida Bay: evidence from C:N:P ratios of the dominant seagrass *Thalassia testudinum. Limnology and Oceanography, 37*(1), 162–171. https://doi.org/10.4319/lo.1992.37.1.0162.

Fry, B. (2002). Conservative mixing of stable isotopes across estuarine salinity gradients: a conceptual framework for monitoring watershed influences on downstream fisheries production. *Estuaries 25*(2): 264-271.

Fry, B. (2006). *Stable Isotope Ecology*. New York: Springer.

Gacia, E., & Duarte, C. M. (2001). Sediment retention by a Mediterranean *Posidonia oceanica* meadow: the balance between deposition and resuspension. *Estuarine, Coastal and Shelf Science*, *52*(4), 505–514. https://doi.org/10.1006/ecss.2000.0753.

Gallegos, M. E., Merino, M., Rodriguez, A., Marbà, N., & Duarte, C. M. (1994). Growth patterns and demography of pioneer Caribbean seagrasses *Halodule wrightii* and *Syringodium filiforme*. *Marine Ecology Progress Series, 109*(1), 99–104.

Gardner W.S., McCarthy, M.J., Soonmo, A., Sobolev, D., Sell, K.S., & Brock, D. (2006). Nitrogen fixation and dissimilatory nitrate reduction to ammonium (DNRA) support nitrogen dynamics in Texas estuaries. *Limnology and Oceanography, 51*(1, part 2), 558–568. https://doi.org/10.4319/lo.2006.51.1_part_2.0558.

Gutierrez, M. A., Cardona, A.A., & Smee, D. L. (2010). Growth patterns of shoal grass *Halodule wrightii* and manatee grass *Syringodium filiforme* in the western Gulf of Mexico. *Gulf and Caribbean Research, 22*(1): 71-75. https://doi.org/10.18785/gcr.2201.09.

Handley, L.L., & Raven, J.A. (1992). The use of natural abundance of nitrogen isotopes in plant physiology and ecology. *Plant, Cell & Environment*, *15*(9), 965–985. https://doi.org/10.1111/j.1365-3040.1992.tb01650.x.

Hayes, J.M. (2004). *An introduction to isotopic calculations*. Woods Hole Oceanographic Institution, Woods Hole, MA.

Hemminga, M.A., & Mateo M.A. (1996). Stable carbon isotopes in seagrasses: variability in ratios and use in ecological studies. *Marine Ecology Progress Series, 140*(1/3), 285–298.

Herzka, S.Z., & K.H. Dunton. (1997). Seasonal photosynthetic patterns of the seagrass *Thalassia testudinum* in the western Gulf of Mexico. *Marine Ecology Progress Series 152*, 103–117. doi:10.3354/meps152103.

Hu, X.P., Burdige, D.J., & Zimmerman, R.C. (2012). $\delta^{13}C$ is a signature of light availability and photosynthesis in seagrass. *Limnology and Oceanography, 57*(2), 441-448. doi: 10.4319/lo.2012.57.2.0441.

Hudak, P. F., & Banks, K. E. (2006). Compositions of first flush and composite storm water runoff in small urban and rural watersheds, north-central Texas. *Urban Water Journal*, *3*(1), 43–49. https://doi.org/10.1080/15730620600578678.

Kaldy, J.E., Cifuentes, L.A., & Brock, D. (2005). Using stable isotope analyses to assess carbon dynamics in a shallow subtropical estuary. *Estuaries* 28(1): 86-95.

Kaldy, J.E., & Dunton, K.H. (2000). Above- and below-ground production, biomass and reproductive ecology of *Thalassia testudinum* (turtle grass) in a subtropical coastal lagoon. *Marine Ecology Progress Series 193*, 271–283. doi:10.3354/meps193271.

Kemp, M.W., Batleson, R., Bergstrom, P., Carter, V., Gallegos, C. L., Hunley, W., … Wilcox, D. J. (2004). Habitat requirements for submerged aquatic vegetation in Chesapeake Bay: water quality, light regime, and physical-chemical factors. *Estuaries*, *27*(3), 363–377. https://doi.org/10.1007/BF02803529.

Kennedy, H., Beggins, J., Duarte, C.M., Fourqurean, J.W., Holmer, M., Marbà, N., & Middelburg, J.J. (2010). Seagrass sediments as a global carbon sink: Isotopic constraints. *Global Biogeochemical Cycles*, *24*(4). https://doi.org/10.1029/2010GB003848.

Kowalski, J.L., DeYoe, H.R., & Allison, T.C. (2009). Seasonal production and biomass of the seagrass, *Halodule wrightii* Aschers. (shoal grass), in a subtropical Texas lagoon. *Estuaries and Coasts*, *32*(3), 467–482. https://doi.org/10.1007/s12237-009-9146-z.

Kuo J. & A.J. McComb. (1998). Cymodoceaceae. In *The Families and Genera of Vascular Plants book series (FAMILIES GENERA, volume 4): Flowering Plants · Monocotyledons, Alismatanae and Commelinanae (except Gramineae).* Edited by K. Kubitzki. Berlin: Springer. 133-140 pp. https://doi.org/10.1007/978-3-662-03531-3.

Lee K.-S., & Dunton K.H. (1999). Inorganic nitrogen acquisition in the seagrass *Thalassia testudinum*: development of a whole-plant nitrogen budget. *Limnology and Oceanography*, *44*(5), 1204–1215. https://doi.org/10.4319/lo.1999.44.5.1204.

Lee, K.-S., Short, F.T., & Burdick, D.M. (2004). Development of a nutrient pollution indicator using the seagrass, *Zostera marina*, along nutrient gradients in three New England estuaries. *Aquatic Botany, 78*(3), 197-216. doi: http://dx.doi.org/10.1016/j.aquabot.2003.09.010.

Lepoint, G., Dauby, P., Fontaine, M., Bouquegneau, J.M., & Gobert, S. (2003) Carbon and nitrogen isotopic ratios of the seagrass *Posidonia oceanica:* depth-related variations. *Botanica Marina 46*, 555–561.

Lepoint, G., Dauby, P., & Gobert, S. (2004). Applications of C and N stable isotopes to ecological and environmental studies in seagrass ecosystems. *Marine Pollution Bulletin*, *49*(11), 887–891. https://doi.org/10.1016/j.marpolbul.2004.07.005.

Lin, G., Banks, T., & Sternberg, L. da S. L. O. (1991). Variation in $\delta^{13}C$ values for the seagrass *Thalassia testudinum* and its relations to mangrove carbon. *Aquatic Botany, 40*(4), 333–341. https://doi.org/10.1016/0304-3770(91)90079-K.

Longley, W. L. (1994). Freshwater inflows to Texas bays and estuaries: ecological relationships and methods for determination of needs. Austin, TX: Texas Water Development Board and Texas Parks and Wildlife Department.

Mahaffey, C., Williams, R.G., Wolff, G.A., Mahowald, N., Anderson, W., & Woodward, M. (2003). Biogeochemical signatures of nitrogen fixation in the eastern North Atlantic. *Geophysical Research Letters, 30*(6). https://doi.org/10.1029/2002GL016542.

Mallette, J. R., Casale, J. F., Jordan, J., Morello, D. R., & Beyer, P. M. (2016). Geographically sourcing cocaine's origin – delineation of the nineteen major coca growing regions in South America. *Scientific Reports, 6*, 23520.

Markert, B.A., Breure, M.A., & Zechmeister, H.G. (2003).Definitions, strategies, and principles for bioindication/biomonitoring. In *Bioindicators & biomarkers:*

principles, concepts, and applications Edited by B.A. Markert, M.A. Breure, & H.G. Zechmeister. Kildington, Oxford, UK: Elsevier.

McClelland, J.W., Valiela, I., & Michener, R.H. (1997). Nitrogen-stable isotope signatures in estuarine food webs: A record of increasing urbanization in coastal watersheds. *Limnology and Oceanography*, *42*(5), 930–937. https://doi.org/10.4319/lo.1997.42.5.0930.

McCready, R.G.L., Gould, W.D., & Barendregt, R.W. (1983). Nitrogen isotope fractionation during the reduction of NO3− to NH4+ by Desulfovibrio sp. *Canadian Journal of Microbiology*, *29*(2), 231–234. https://doi.org/10.1139/m83-038.

McLeod, E., Chmura, G.L., Bouillon, S., Salm, R., Bjork, M., Duarte, C.M., . . . Silliman, B.R. (2011). A blueprint for blue carbon: toward an improved understanding of the role of vegetated coastal habitats in sequestering CO_2. *Frontiers in Ecology and the Environment, 9*(10), 552-560. doi: 10.1890/110004.

McPherson, M.L., Zimmerman, R.C., & Hill, V.J. (2015). Predicting carbon isotope discrimination in Eelgrass (*Zostera marina* L.) from the environmental parameters—light, flow, and [DIC]. *Limnology and Oceanography, 60*(6), 1875–1889. https://doi.org/10.1002/lno.10142.

Möbius, J. (2013). Isotope fractionation during nitrogen remineralization (ammonification): Implications for nitrogen isotope biogeochemistry. *Geochimica et Cosmochimica Acta*, *105*, 422–432. https://doi.org/10.1016/j.gca.2012.11.048.

Montefalcone, M. (2009). Ecosystem health assessment using the Mediterranean seagrass Posidonia oceanica: A review. *Ecological Indicators*, *9*(4), 595-604. doi: 10.1016/j.ecolind.2008.09.013.

Mooney, R.F., & McClelland, J.W. (2012). Watershed export events and ecosystem responses in the Mission–Aransas National Estuarine Research Reserve, south Texas. *Estuaries and Coasts*, *35*(6), 1468–1485. https://doi.org/10.1007/s12237-012-9537-4.

Nikolenko, O., Jurado, A., Borges, A. V., Knöller, K., & Brouyère, S. (2018). Isotopic composition of nitrogen species in groundwater under agricultural areas: a review. *Science of The Total Environment*, *621*, 1415–1432. https://doi.org/10.1016/j.scitotenv.2017.10.086

Ondiviela, B., Losada, I.J., Lara, J.L., Maza, M., Galván, C., Bouma, T.J., & van Belzen, J. (2014). The role of seagrasses in coastal protection in a changing climate. *Coasts@Risks: THESEUS, a New Wave in Coastal Protection*, *87*, 158–168. https://doi.org/10.1016/j.coastaleng.2013.11.005.

Onuf, C.P. (2007). Laguna Madre. In *Seagrass status and trends in the northern Gulf of Mexico: 1940-2002*. Edited by Handley, L., Altsman, D., & DeMay, R. Reston, VA: U.S. Geological Survey.

Orth, R. J., Carruthers, T.J.B., Dennison, W.C., Duarte, C.M., Fourqurean, J.W., Heck, K.L., … Williams, S.L. (2006). A global crisis for seagrass ecosystems. *BioScience*, *56*(12), 987–996. https://doi.org/10.1641/0006-3568(2006)56[987:AGCFSE]2.0.CO;2.

Papadimitriou S., Kennedy H., Kennedy D.P., & Borum J. (2005). Seasonal and spatial variation in the organic carbon and nitrogen concentration and their stable isotopic composition in *Zostera marina* (Denmark). *Limnology and Oceanography, 50*(4), 1084–1095. https://doi.org/10.4319/lo.2005.50.4.1084.

Parmar, T.K., Rawtani, D., & Agrawal, Y. K. (2016). Bioindicators: the natural indicator of environmental pollution. *Frontiers in Life Science, 9*(2), 110–118. https://doi.org/10.1080/21553769.2016.1162753.

Parnell, A.C., Inger, R., Bearhop, S., & Jackson, A.L. (2010). Source partitioning using stable isotopes: coping with too much variation. *PLoS One, 5*(3), e9672. doi: 10.1371/journal.pone.0009672.

Pellegrini, M., Pouncett, J., Jay, M., Pearson, M.P., & Richards, M.P. (2016). Tooth enamel oxygen "isoscapes" show a high degree of human mobility in prehistoric Britain. *Scientific Reports, 6*, 34986.

Peterson, B. J., & Fry, B. (1987). Stable isotopes in ecosystem studies. *Annual Review of Ecology and Systematics, 18*(1), 293–320. https://doi.org/10.1146/annurev.es.18.110187.001453.

Peterson, C.H., Luettich, R.A. Jr., Micheli, F., & Skilleter, G.A. (2004). Attenuation of water flow inside seagrass canopies of differing structure. *Marine Ecology Progress Series, 268*, 81–92.

Planavsky, N.J., Partin, C., & Bekker, A. (2011). Carbon isotopes as a geochemical tracer. In *Encyclopedia of Astrobiology*. Edited by M. Gargaud, R. Amils, J.C. Quintanilla, H.J. Cleaves, W.M. Irvine, D. Pinti, & M. Viso. Berlin: Springer-Verlag. 249-253 pp.

Pulich, W.M. (1985). Seasonal growth dynamics of *Ruppia maritima* L. sl. and *Halodule wrightii* Aschers. in southern Texas and evaluation of sediment fertility status. *Aquatic Botany, 23*: 53–66. doi: 10.1016/0304-3770(85)90020-8.

Pulich, W. Jr., & Rabalais, S. (1986). Primary production potential of blue-green algal mats on southern Texas tidal flats. *The Southwestern Naturalist 31*(1):39-47.

Pulich, W.M. Jr., & Scalan, R.S. (1987). Organic carbon and nitrogen flow from marine Cyanobacteria to semiaquatic insect food webs. *Contributions in Marine Science 30*, 27-37.

Reyna, N. E., Hardison, A. K., & Liu, Z. (2017). Influence of Major Storm Events on the Quantity and Composition of Particulate Organic Matter and the Phytoplankton Community in a Subtropical Estuary, Texas. *Frontiers in Marine Science*, *4*, 43. https://doi.org/10.3389/fmars.2017.00043.

Robinson, D. (2001). $\delta^{15}N$ as an integrator of the nitrogen cycle. *Trends in Ecology & Evolution*, *16*(3), 153–162. https://doi.org/10.1016/S0169-5347(00)02098-X.

Santschi, P.H., Oktay, S.D., & Cifuentes, L. (2007). Carbon isotopes and iodine concentrations in a Mississippi River delta core recording land use, sediment transport, and dam building in the river's drainage basin. *Marine Environmental Research*, *63*(3), 278–290. https://doi.org/10.1016/j.marenvres.2006.11.002.

Short, F.T. (1987). Effects of sediment nutrients on seagrasses: literature review and mesocosm experiment. *Aquatic Botany 27*, 41–57. doi:10.1016/0304-3770(87)90085-4.

Texas Parks and Wildlife (TPWD). (1999). Seagrass conservation plan for Texas. Austin, TX: TPWD Resource Protection Division.

Texas Seagrass Monitoring Program. (2018). <http://www.texasseagrass.org/>.

Texas Water Development Board. (2017). Drought and drought response in Texas. In *2017 State Water Plan.* Austin, TX: Texas Water Development Board. 30-39 pp.

Tieszen, L. L. (1991). Natural variations in the carbon isotope values of plants: Implications for archaeology, ecology, and paleoecology. *Journal of Archaeological Science*, *18*(3), 227–248. https://doi.org/10.1016/0305-4403(91)90063-U.

Touchette, B.W., & Burkholder, J.M. (2000). Overview of the physiological ecology of carbon metabolism in seagrasses. *Journal of Experimental Marine Biology and Ecology*, *250*(1), 169–205. https://doi.org/10.1016/S0022-0981(00)00196-9.

Tunnell, J.W. & F.W. Judd. 2002. *The Laguna Madre of Texas and Tamaulipas*. College Station, TX: Texas A&M University Press.

Unkovich, M. (2013). Isotope discrimination provides new insight into biological nitrogen fixation. *New Phytologist*, *198*(3), 643–646. https://doi.org/10.1111/nph.12227.

Welsh, D.T. (2000). Nitrogen fixation in seagrass meadows: Regulation, plant–bacteria interactions and significance to primary productivity. *Ecology Letters*, *3*(1), 58–71. https://doi.org/10.1046/j.1461-0248.2000.00111.x.

Wilson, S. S. and K.H. Dunton. (2017). Hypersalinity during regional drought drives mass mortality of the seagrass *Syringodium filiforme* in a subtropical lagoon. *Estuaries and Coasts*: in press. DOI 10.1007/s12237-017-0319-x.

Xue, D., Botte, J., De Baets, B., Accoe, F., Nestler, A., Taylor, P., . . . Boeckx, P. (2009). Present limitations and future prospects of stable isotope methods for nitrate source identification in surface- and groundwater. *Water Res, 43*(5), 1159-1170. doi: 10.1016/j.watres.2008.12.048.

Yamamuro, M., Kayanne, H., & Yamano, H. (2003). $\delta^{15}N$ of seagrass leaves for monitoring anthropogenic nutrient increases in coral reef ecosystems. *Marine Pollution Bulletin*, *46*(4), 452–458. https://doi.org/10.1016/S0025-326X(02)00463-0.